

# **Mapping of Human Hereditary Skeletal Dysplasia**

## **Candidate Genes in Consanguineous Families**



**By**

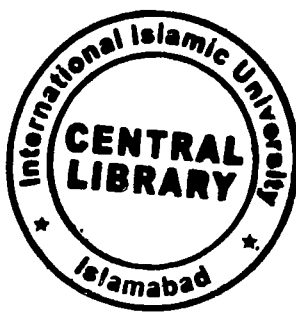
**YASMIN HASHIM**

**Department of Bioinformatics & Biotechnology**

**Faculty of Basic and Applied Sciences**

**International Islamic University Islamabad**

**(2016)**



TH-16124

M. M. M.

MS

576 50285

YAM



# **Mapping of Human Hereditary Skeletal Dysplasia Candidate Genes in Consanguineous Families**



**YASMIN HASHIM**

**60-FBAS/MSBT/S13**

**Supervisor**

**Dr. Shaheen Shahzad**

**Assistant Professor**

**IIUI**

**Co-supervisor**

**Dr. Abdul Hameed**

**Principal scientific officer**

**IBGE (KRL)**

**Department of Bioinformatics & Biotechnology**

**Faculty of Basic and Applied Sciences**

**International Islamic university Islamabad**

**(2016)**

**Department of Bioinformatics and Biotechnology  
International Islamic University Islamabad**

**FINAL APPROVAL**

It is certified that we have read the thesis submitted by Ms. Yasmin Hashim and it is our judgment that this project is of sufficient standard to warrant its acceptance by the International Islamic University, Islamabad for the MS Degree in Biotechnology.

**COMMITTEE**

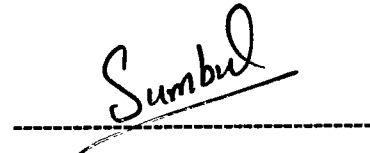
**External Examiner**

Dr. Naeem  
Associate Professor  
Quaid-i-Azam University



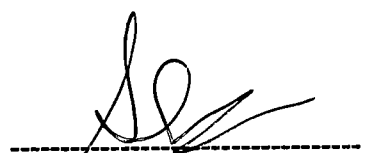
**Internal Examiner**

Dr. Sumbul Khalid  
Assistant Professor  
International Islamic University, Islamabad.



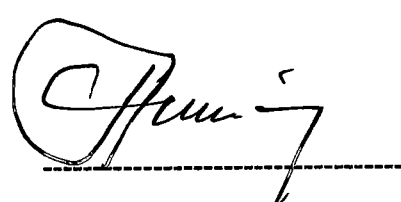
**Supervisor**

Dr. Shaheen Shahzad  
Assistant Professor  
International Islamic University, Islamabad



**Co-Supervisor**

Dr. Abdul Hameed  
Principal scientific officer  
IBGE-KRL



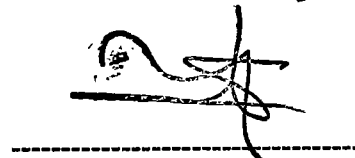
**Head of Department**

Dr. Naveeda Riaz  
Associate Professor  
International Islamic University, Islamabad.



**Dean FBAS**

Dr. Muhammad Sher



**A Thesis Submitted to Department of Bioinformatics and  
Biotechnology,**

**International Islamic University, Islamabad**

**As a partial fulfillment of requirement for the award of the  
degree of**

**MS in Biotechnology**

Dedicated to

---

My Parents

Who's Love and Prayers Always  
Accompanied Me

And

My Husband

Who Always Look Forward for My  
Success

## **DECLARATION**

I hereby declare that the present work in the following thesis is my own effort except, where otherwise acknowledged and that the thesis is my own composition. No part of the thesis has been previously presented for any other degree.

Date 18.03.2016



**Yasmin Hashim**

**60-FBAS/MSBT-S13**

# CONTENTS

	<u>Page No.</u>
<b>ACKNOWLEDGMENT</b>	<b>i</b>
<b>LIST OF ABBREVIATIONS</b>	<b>ii</b>
<b>LIST OF FIGURES</b>	<b>iv</b>
<b>LIST OF TABLES</b>	<b>viii</b>
<b>ABSTRACT</b>	<b>ix</b>
<b><i>CHAPTER-1</i></b>	
<b>INTRODUCTION</b>	<b>1</b>
1.1 Skeletal Dysplasias	1
1.1.1 Osteodysplasias	1
1.1.2 Chondrodysplasias	2
1.1.3 Dysostoses	2
1.1.4 Reduction	2
1.2. Diagnostic Approaches For Skeletal Dysplasias	2
1.3. Classification of Skeletal Dysplasias	3
1.3.1. FGFR3 Chondrodysplasia Group disorders	3
1.3.1.1. <i>FGFR3</i> Gene	3
1.3.1.2. Achondroplasia (ACH)	4
1.3.1.2.1. Diagonosis of ACH	4
1.3.1.2.2. Strategies for treating ACH	5
1.3.1.2.2.1. FGFR3 kinase inhibitors	5
1.3.1.2.2.2. Monoclonal antibodies	5
1.3.1.2.2.3. RNAi	5
1.3.1.2.2.4. Hsp90 inhibition	6
1.3.1.2.2.5. Other therapeutic approaches	6
1.3.1.3. Hypochondroplasia	6
1.3.1.4. Thanatophoric dysplasia (TD)	7
1.3.1.4.1. Thanatophoric dysplasia Type I (TDI)	7
1.3.1.4.2. Thanatophoric dysplasia Type II (TDII)	7
1.3.1.5. SADDAN dysplasia	8
1.3.1.6. Craniosynostosis disorders	8
1.3.1.6.1. Muenke coronal craniosynostosis	8
1.3.1.6.2. Crouzon syndrome with acanthosisnigricans	8
1.3.2. Scoliosis	10
1.3.2.1. Classification of Scoliosis	10

---

1.3.2.1.1. Congenital	10
1.3.2.1.2. Neuromuscular	10
1.3.2.1.3. Syndrome-related	10
1.3.2.1.4. Idiopathic Scoliosis (IS)	
1.3.2.1.4.1 Classification of IS	
1.3.2.1.5. Nonstructural	11
1.3.2.1.6. Structural	11
1.3.2.2. Adolescent idiopathic scoliosis (AIS)	11
1.3.2.2.1. Prevalence	11
1.3.2.2.2. Symptoms	12
1.3.2.2.3. Diagnosis of AIS	12
1.3.2.2.4. Treatment of AIS	12
1.3.2.2.5. Idiopathic scoliosis related Genes	13
1.4. Objectives	16

**CHAPTER-2**

<b>MATERIALS AND METHODS</b>	17
2.1. Study Subject	17
2.2. Families History and Analysis	17
2.3. Pedigree Construction and Interpretation	17
2.4. Blood acquisition	17
2.5. Extraction of Genomic DNA	18
2.5.1. Phenol-Chloroform Method	18
2.6. DNA Concentration and purity determination	20
2.7. DNA Integrity	20
2.8. Polymerase Chain Reaction	20
2.9. Linkage Analysis	21
2.10. Gel Electrophoresis	21
2.10.1. Polyacrylamide Gel Electrophoresis (PAGE)	21

**CHAPTER-3**

<b>RESULTS</b>	24
3.1. Family-A	24
3.2. Family-B	24
3.3. Mapping Genes Involved in Achondroplasias	24
3.4. Mapping Genes Involved Adolescent Idiopathic Scoliosis	25

**CHAPTER-4**

Discussion	60
------------	----

**CHAPTER-5**

References	62
------------	----

### ACKNOWLEDGEMENTS

All praises and glories to *Almighty Allah* who says in the Holy Quran, "And your Lord is the most gracious who taught by the pen. Taught man (those things) which he did not know". Countless Daroo on the Prophet of mercy *HAZRAT MUHAMMAD (Sall-Allah-Ho-Alaihay-Wa-Aalayhi-Wasallam)*, who showed the path of knowledge to the mankind and gave the lessons of seeking knowledge from cradle to the grave.

The efforts put forth in this research are just because of my supervisor Dr. Shaheen shahzad, who guided and encouraged me in a best way throughout study. I would like to express my gratitude to my co-supervisor Dr. Abdul Hameed (Institute of biomedical and genetic engineering) who helped me a lot and provided me invaluable assistance, support and guidance to complete this research work. On this occasion I present my heartfelt thanks to the International Islamic University ,Islamabad, for facilitating me in doing my research work. Special thanks to the all the affected families for their cooperation in the research work, May Allah Almighty relieve their pain.

It is indeed ineffable to mention my appreciation to my loving father for his unstinting support, encouragement and guidance which made me able to achieve this goal. Besides, the love of my sweet mother proved a beacon of light at every step of my life. I am unable to find any words which can express my feelings of thanks for my Husband for his valuable support and encouragement.

May Allah succeed all of us in our good and noble aims and empower us to serve mankind. (*Ameen*)

*Yasmin Hashim*

**LIST OF ABBREVIATIONS**

FGFR3	Fibroblast growth factor receptor 3 gene
SADDAN	Severe achondroplasia with developmental delay and acanthosisnigricans
ISDS	International skeletal dysplasia society
INCDB	International nomenclatures of constitutional diseases of bones
FGFR	Fibroblast growth factor receptor
Lys	Lysine
OI	Osteogenesis imperfect
MPS	Mucopolysaccharidosis
TD	Thanatophoric dysplasia
Met	Methionine
Ala	Alanine
Glu	Glutamine
AIS	Adolescent Idiopathic Scoliosis
Kb	Kilo base
cDNA	Complementary deoxyribonucleic acid
GNS	N-acetyl glucosamine 6-sulfatase
ml	Milliliter
DNA	Deoxy ribonucleic acid
EDTA	Ethylene diamine tetra-acetic acid
ml	Microliter
mM	Milli molar
pH	Negative log of hydrogen ions concentration
MgCl <sub>2</sub>	Magnesium chloride
v/v	Volume by volume
Rpm	Revolution per minute
Mg	Milli gram
C	Degree centigrade

M	Molar
%	Percentage
OD	Optical density
Nm	Nano meter
UV	Ultraviolet
PCR	Polymerase chain reaction
pmol	Pico mole
Taq	Thermus aquaticus
dNTP's	Deoxy nucleotide triphosphates
(NH4)2SO4	Ammonium sulphate
NCBI	National center for biotechnology information
Gm	Gram
Bp	Base pair
PAGE	Polyacrylamide gel electrophoresis
APS	Ammonium persulphate
TEMED	N, N, N', N'-Tetra methylethylene diamine
Mm	Milli meter
Ta	Annealing temperature
Tris	Hydroxymethyl aminomethane
HCl	Hydrochloric acid
NaCl	Sodium chloride
RR	Ready reaction mix
Cm	Centi meter
Asn	Asparagine
cM	Centi morgan
SDS	Sodium dodesyl sulfate

**LIST OF FIGURES**

<b><u>Figure No.</u></b>	<b><u>Titles</u></b>	<b><u>Page No.</u></b>
<b>Figure 1.1</b>	A putative model for FGFR3 signaling.	9
<b>Figure 3.1</b>	Pedigree drawing of the family A segregating autosomal recessive Achondroplasias	26
<b>Figure 3.2</b>	(a) An affected male individual (IV-1) of family A: (b) Affected of female IV-4 of family A:	27
<b>Figure 3.3</b>	Pedigree drawing of the family B segregating Adolescent idiopathic scoliosis	28
<b>Figure 3.4</b>	An affected individuals of family B. (a) Showing AIS in an affected male (IV;1) (b) showing AIS in an affected male (IV-2),(c) showing AIS in an female (IV-8).	29
<b>Figure 3.5</b>	Electropherogram showing allele pattern obtained with marker D4S2936in family A	31
<b>Figure 3.6</b>	Electropherogram showing allele pattern obtained with marker D4S43in family A	31
<b>Figure 3.7</b>	Electropherogram showing allele pattern obtained with marker D4S127in family A	32
<b>Figure 3.8</b>	Electropherogram showing allele pattern obtained with marker D4S179in family A	32
<b>Figure 3.9</b>	Electropherogram showing allele pattern obtained with marker D4S2957 in family A	33
<b>Figure 3.10</b>	Electropherogram showing allele pattern obtained with marker D4S3023in family A	33
<b>Figure 3.11</b>	Electropherogram showing allele pattern obtained with marker D4S2925in family A	34
<b>Figure 3.12</b>	Electropherogram showing allele pattern obtained with marker D4S394in family A	34
<b>Figure 3.13</b>	Electropherogram showing allele pattern obtained with marker D9S1678in family A	35
<b>Figure 3.14</b>	Electropherogram showing allele pattern obtained with marker D9S319 in family A	35

<b>Figure 3.15</b>	Electropherogram showing allele pattern obtained with marker D9S1118in family A	36
<b>Figure 3.16</b>	Electropherogram showing allele pattern obtained with marker , D9S1817in family A	36
<b>Figure 3.17</b>	Electropherogram showing allele pattern obtained with marker D9S1874in family A	37
<b>Figure 3.18</b>	Electropherogram showing allele pattern obtained with marker D9S55in family A	37
<b>Figure 3.19</b>	Electropherogram showing allele pattern obtained with marker D9S773in family A	38
<b>Figure 3.20</b>	Electropherogram showing allele pattern obtained with marker D9S1110in family A	38
<b>Figure 3.21</b>	Electropherogram showing allele pattern obtained with marker D9S50 in family A	39
<b>Figure 3.22</b>	Electropherogram showing allele pattern obtained with marker D9S229 in family A	39
<b>Figure 3.23</b>	Electropherogram showing allele pattern obtained with marker D9S1879 in family A	40
<b>Figure 3.24</b>	Electropherogram showing allele pattern obtained with marker D9S15 in family A	40
<b>Figure 3.25</b>	Electropherogram showing allele pattern obtained with marker D9S1806 in family A	41
<b>Figure 3.26</b>	Electropherogram showing allele pattern obtained with marker D9S1876in family A	41
<b>Figure 3.27</b>	Electropherogram showing allele pattern obtained with marker D2S213n family A	42
<b>Figure 3.28</b>	Electropherogram showing allele pattern obtained with marker D2S396 in family A	42
<b>Figure 3.29</b>	Electropherogram showing allele pattern obtained with marker D2S42317in family A	43
<b>Figure 3.30</b>	Electropherogram showing allele pattern obtained with marker D2S427in family A	43
<b>Figure 3.31</b>	Electropherogram showing allele pattern obtained with marker D2S2344in family A	44

---

<b>Figure 3.32</b>	Electropherogram showing allele pattern obtained with marker D19S894 in family B	44
<b>Figure 3.33</b>	Electropherogram showing allele pattern obtained with marker D19S1034 in family B	45
<b>Figure 3.34</b>	Electropherogram showing allele pattern obtained with marker D19S567 in family B	45
<b>Figure 3.35</b>	Electropherogram showing allele pattern obtained with marker D19S884 in family B	46
<b>Figure 3.36</b>	Electropherogram showing allele pattern obtained with marker D19S916 in family B	46
<b>Figure 3.37</b>	Electropherogram showing allele pattern obtained with marker D19S865 in family B	47
<b>Figure 3.38</b>	Electropherogram showing allele pattern obtained with marker D19S221 in family B	47
<b>Figure 3.39</b>	Electropherogram showing allele pattern obtained with marker D17S1856 in family B	48
<b>Figure 3.40</b>	Electropherogram showing allele pattern obtained with marker D17S2839 in family B	48
<b>Figure 3.41</b>	Electropherogram showing allele pattern obtained with marker D17S1843 in family B	49
<b>Figure 3.42</b>	Electropherogram showing allele pattern obtained with marker D17S2196 in family B	49
<b>Figure 3.43</b>	Electropherogram showing allele pattern obtained with marker D17S842 in family B	50
<b>Figure 3.44</b>	Electropherogram showing allele pattern obtained with marker D17S783 in family B	50
<b>Figure 3.45</b>	Electropherogram showing allele pattern obtained with marker D17S1878 in family B	51
<b>Figure 3.46</b>	Electropherogram showing allele pattern obtained with marker D17S1800 in family B	51
<b>Figure 3.47</b>	Electropherogram showing allele pattern obtained with marker D8S1471 in family B	52
<b>Figure 3.48</b>	Electropherogram showing allele pattern obtained with marker D8S565 in family B	52

<b>Figure 3.49</b>	Electropherogram showing allele pattern obtained with marker D8S592 in family B	53
<b>Figure 3.50</b>	Electropherogram showing allele pattern obtained with marker D8S527 in family B	53
<b>Figure 3.51</b>	Electropherogram showing allele pattern obtained with marker D8S199 in family B	54
<b>Figure 3.52</b>	Electropherogram showing allele pattern obtained with marker D9S1105 in family B	54
<b>Figure 3.53</b>	Electropherogram showing allele pattern obtained with marker D9S1776 in family B	55
<b>Figure 3.54</b>	Electropherogram showing allele pattern obtained with marker D9S1685 in family B	55
<b>Figure 3.55</b>	Electropherogram showing allele pattern obtained with marker D9S290 in family B	56
<b>Figure 3.56</b>	Electropherogram showing allele pattern obtained with marker D9S766 in family B	56
<b>Figure 3.57</b>	Electropherogram showing allele pattern obtained with marker D9S1793 in family B	57
<b>Figure 3.58</b>	Electropherogram showing allele pattern obtained with marker D17S1847 in family B	57
<b>Figure 3.59</b>	Electropherogram showing allele pattern obtained with marker D17S1806 in family B	58
<b>Figure 3.60</b>	Electropherogram showing allele pattern with marker D17S784 in family B.	58
<b>Figure 3.61</b>	Electropherogram showing allele pattern with marker D17S914 in family B.	59
<b>Figure 3.62</b>	Electropherogram showing allele pattern with marker D17S668 in family B.	59

**LIST OF TABLES**

<b><u>Table No.</u></b>	<b><u>Title</u></b>	<b><u>Page No.</u></b>
<b>Table 2.1.</b>	Composition of solutions	<b>19</b>
<b>Table 2.2.</b>	List of microsatellite markers used to test linkage to genes involved in Achondroplasias	<b>22</b>
<b>Table 2.3.</b>	List of microsatellite markers used to test linkage to genes involved in Adolescent Idiopathic scoliosis	<b>23</b>

**ABSTRACT**

Skeletal dysplasias are a heterogeneous group of diseases characterized by generalized structural abnormality of bone and cartilage growth. A number of growth and morphogenetic factors that regulate osteoblast and osteoclast activity are involved in bone development and modeling. Mutations in genes encoding these proteins result in clinically diverse and genetically heterogeneous group of genetic disorders, collectively known as skeletal dysplasias. There has been substantial progress in identification of molecular defects responsible for skeletal deformities and the genetic defects in 316 out of 456 conditions included in skeletal dysplasias have been associated with mutations in one or more of 226 different genes. The inheritance fashion in skeletal dysplasias may be autosomal dominant, autosomal recessive, or X-linked. The frequency of skeletal disorders increases with successive intermarriages in a generation. In Pakistani population consanguineous marriages are common due to social, ethnic and traditional customs.

In the present study two families (A and B) showing clinically distinct autosomal recessive hereditary skeletal dysplasias were evaluated genetically. Affected individuals of family A showed autosomal recessive achondroplasia, with no other associated abnormality. In family B the affected individuals showed autosomal recessive Idiopathic scoliosis. Technique of homozygosity mapping was used to track the gene responsible for autosomal recessive skeletal dysplasias in both families. In homozygosity mapping with polymorphic microsatellite markers, family A and B were excluded from the known loci involved in Achondroplasia and Adolescent Idiopathic scoliosis respectively which signifies the involvement of a novel gene in causing skeletal dysplasias in both these families.

Attempt to identify the novel gene responsible for Achondroplasia and Adolescent Idiopathic scoliosis will shed light on the mechanism of pathogenesis and subsequently open the way for effective treatment of these skeletal disorders.

# **CHAPTER 1**

# **INTRODUCTION**

## INTRODUCTION

The human skeleton is an endoskeleton composed of bones (206), cartilage and three types of cells, osteoblasts, osteoclasts and chondrocytes. Bone is a type of mineralized connective tissue that undergoes a process of renewing. During this process, old bones are destroyed and new ones are formed. Cartilage is an elastic type of connective tissue that constitutes the parts of the skeleton that can't be totally rigid, due to the necessity of body movements (Savarirayan and Rimoin, 2002). The human skeletal system has two sub division, axial and appendicular skeleton. The axial skeleton consists of 80 bones, that includes bones of skull, vertebral column and thoracic cage. The appendicular skeleton comprises of 126 bones of upper and lower limbs as well as pelvic and pectoral girdles

Besides supporting the organism, Skeletal System is responsible for other important functions. The major ones are:

- Provides protection to vital internal organs;
- Serve as mechanical base of the movement;
- Storage reservoir of essential minerals, as calcium and magnesium;
- Hematopoietic organ - continuous production of blood cells.

(Kornak and Mundlos.,2003).

### 1.1 SKELETAL DYSPLASIA

The skeletal dysplasia are a heterogeneous group of genetic disorders characterized by abnormal development of bone and cartilage. The pattern of inheritance of skeletal dysplasia can be autosomal dominant, autosomal recessive, or X linked disorders. Although individually rare, prevalence rates of the skeletal dysplasia at birth is estimated to be 1/5000 live births. They manifest with short stature (mainly disproportionate), neurological complications, degenerative joint disease, abnormalities in development and maintenance of appendicular and axial skeleton (Ornitz and Marie., 2002). The clinical severity ranges from relatively mild to severe and lethal conditions. These disorders can be divided into four main groups.

#### 1.1.1. OSTEODYSPASIA

The osteodysplasia is characterized either by osteosclerosis or osteopenia, in osteosclerosis, abnormal increase in the density of bone tissue occurs, where as osteopenia

is characterized by lower bone mineral density (Hurst *et al.*, 2005).

### **1.1.2. Chondrodysplasia**

The chondrodysplasia is characterized by abnormality in development of cartilage especially at ends of long bones results in short stature dwarfism (Mortier, 2001).

### **1.1.3. Dysostoses**

Dysostoses is malformations of single bones or in combination, because of abnormal ossification. These disorders include polydactyl, syndactyly and Triphalangism (Zelzer and Olson, 2003).

### **1.1.4. Reduction**

Reduction is referred to a condition in which a secondary malformation of bones takes place (Schramm *et al.*, 2009).

## **1.2. Diagnostic Approaches for Skeletal Dysplasia**

Diagnosis of skeletal dysplasia is based on radiographic, biochemical, clinical, and molecular criteria. However molecular mechanisms have improved clinical diagnosis and providing reproductive choices for patients and their families (Jane *et al.*, 2005).

### **Clinical examination**

In the differential diagnosis of skeletal disorders, the short stature is observed, whether it is proportionate or disproportionate. The proportionate short stature shows that condition is due to non-skeletal dysplasia defects like endocrine or metabolic disorders. While patients of skeletal dysplasia have disproportionate short stature. In clinical examination, various features like patient age at disease onset, malformed features, specific skeletal deformations and inheritance of the disorder should be investigated.

### **Radiology**

Radiographic investigation is of major importance in defining the skeletal disease. Bone density should be examined, decreased or increased changes should be noted. Initial location of the shortening of the limb, Metaphyseal, diaphysela, epiphyseal

irregularity and vertebral column shape should be determined. In addition biochemical analysis of blood and tissue samples such as cartilage or bone should be performed (Tuysuz.,2004).

### 1.3 CLASSIFICATION OF SKELETAL DYSPLASIAS

In most osteochondrodysplasia there is a generalized abnormality in linear skeletal growth and in some disorders there are concomitant abnormalities in organ systems other than the skeleton. Mutations responsible for skeletal dysplasia may cause defects, in the synthesis of structural proteins and in metabolic pathways, degradation of macromolecules, growth factors, receptors and transcription factors. (Deborah *et al.*,2009). In the 1960, heterogeneity of genetic skeletal disorders encouraged a team of professionals to organize a nomenclature called “Constitutional (or intrinsic) disorders of bone”. Revisions have been made in 1977, 1983, 1992, and 1997. Earlier, the classification of skeletal disorder were purely clinical. Later, pathogenetic information of various phenotypes had enabled spranger (1992) to classified 200 different skeletal dysplasia phenotypes on the basis of clinical, radiological and molecular criteria. International Skeletal Dysplasia Society (ISDS) was established in 1999 to deal with the growing complexity of information and to guarantee a proper clinical, radiological and molecular representation of skeletal dysplasia. Hence the need to develop a standardized classification and nomenclature system led to the foundation of INCDB (International Nomenclatures of Constitutional Diseases of Bones) (Mortier., 2001). According to recent classification of skeletal dysplasia 456 different conditions were documented and placed in 40 groups according to their molecular, biochemical and radiographic evaluation. Out of them 316 were identified to be cause by mutations in one or more of 226 different genes. These 40 groups are placed under ten large families (Warman *et al.*, 2010).

#### 1.3.1 FGFR3 Chondrodysplasia Group of Disorders

##### 1.3.1.1 FGFR-3 gene

The *FGFR3* gene is located on chromosome 4p16.3 that encodes for a protein, the fibroblast growth factor receptor 3. In humans FGFR-3 represents a member of trans membrane tyrosine kinases receptor family containing 4 major FGF receptors (FGFR1–4)

that bind fibroblast growth factors (FGFs) with variable affinity (Colvin *et al.*, 1996). A full-length FGFR protein consists of a glycosylated extracellular region composed of three immunoglobulin-like domains, a single hydrophobic transmembrane segment and a cytoplasmic tyrosine kinase domain. The FGFR3 gene contains 19 exons and 18 introns. The FGFR3 gene is spanning 16 kb, comprises of 11 kb intronic region, 4.2 kb of exonic sequences, and 1.5 kb of the 5'-untranslated region (Ana *et al.*, 1997). Ligand binding leads to dimerization of two monomeric FGFRs as a result phosphorylation of tyrosine residues occurs and starts a cascade of signaling mechanism that ultimately influences skeletal development through regulation of cartilage growth, as shown in Figure 1.1 (Vajo *et al.*, 2000). In different tissues and in different developmental stage, variety of dimers combinations are possible, this diversity plays an important role in skeletal differentiation. FGFR3 is actually negative regulator of skeletal growth, which restricts the length of the epiphyseal plates of long bones via inhibition of chondrocyte proliferation (Richette *et al.*, 2008). The role of the *FGFR3* (MIM# 134934) in bone development was revealed in 1994, when Shiang *et al.* reported a mutation in FGFR3 in achondroplasia patient (Shiang *et al.*, 1994). FGFR3 chondrodysplasia group of disorders are;

### 1.3.1.2 Achondroplasia

Achondroplasia (ACH; MIM# 100800) is the most common type of dwarfism with a prevalence rate 1:15,000 to 1:40,000 live births. It is an autosomal dominant disorder that results from a de novo mutation in The *FGFR3* gene. It is characterized by short stature with disproportionately short limbs, macrocephaly, three pronged fingers (trident) and characteristic facial features with depressed nasal bridge, frontal bossing and mid-face hypoplasia (Trotter and Hall, 2005). Most individuals with ACH have a G-to-A transition mutation at nucleotide 1138 of the *FGFR3* gene. In the same nucleotide G>C transversion was also identified. These mutations result in substitution of arginine for a glycine residue at position 380 (Gly380Arg) in the *FGFR3* protein. (Vajo *et al.*, 2000; Heuertz *et al.*, 2006).

#### 1.3.1.2.1 Diagnosis of ACH

ACH can be diagnosed on the basis of physical, radiographic and histopathology findings. Characteristic features of ACH can be determined by X-rays, ultrasound and other imaging techniques. With the help of ultrasound imaging, the ACH can be diagnosed before birth.

Specific characteristics of achondroplasia are detectable during pregnancy using ultrasound and genetic tests, like abnormally large head size of infant. If doctor suspects achondroplasia, genetic tests may be performed. These tests look for the defective FGFR3 gene in a sample of amniotic fluid. However ACH after birth can be diagnosed by using blood tests and by X-ray to examine length of child bone (Martinez *et al.*, 2010).

### **1.3.1.2.2. Strategies for treating Achondroplasia**

#### **1.3.1.2.2.1. FGFR3 kinase inhibitors**

This approach is based on fact that FGFR3's kinase activity is important for its activation and signaling, as a result chemical inhibition kinase activity has been purposed to block FGFR3 inhibitory effects and regain normal skeletal development. It has been successful for cancer therapy, but in case of ACH treatment there is problem of cross reactivity, Because of similarity in tyrosine kinase domain structure in all receptor tyrosine kinase (RTK) sub families, so chemicals for kinase inhibition of FGFR3 also inhibits other RTKs. Consequently Aviezer *et al.* reported synthesis of FGFR3 selective inhibitors. The chemical inhibitor restore normal limb bones growth in cultured knock-in mouse of achondroplasia. However, this approach has not been reported in live mice (Laederich and Horton ,2012).

#### **1.3.1.2.2.2 Monoclonal antibodies**

This approach is purposed ,after the treatment of breast cancer patients with monoclonal antibody ( trastuzumab). Trastuzumab binds to the HER2 and reverses its adverse effects on cancer cells. However, there are reports on synthesis of FGFR3 specific antibody to prevent its ligand-induced activation however, but successful stimulation of bone growth in vivo has not been yet tested. Activating FGFR3 mutations promote proliferation of the tumour cells in bladder cancer. However blocking antibodies effectively prevents tumour cells proliferation, provide evidences regarding usefulness of this strategy in treatment of Achondroplasia (Laederich and Horton , 2012).

#### **1.3.1.2.2.3 RNAi**

The basic purpose of RNAi technique to use here, is to prevent the expression of FGFR3 mutated gene by inhibition of its mRNA transcripts translation. RNAi initiated by micro RNAs (miRNAs), that join up to form short RNA duplexes. These duplexes

along with RNA-induced silencing complexes binds to and inhibit target transcripts. This process can also be triggered by artificial RNA that mimics endogenous miRNA, that are known as siRNA (small interfering RNA). So expression of any gene can be prevented by designing specific artificial RNA. The clinical application of RNAi in achondroplasia is to specifically block mutant FGFR3 allele, while leaving normal FGFR3 allele. As many clinical trials for Achondroplasia are underway, but still some issues need to be addressed, such as method of siRNA delivery and stability of siRNA and to ensure selective silencing of mutant allele (Laederich and Horton., 2012).

#### **1.3.1.2.2.4. Hsp90 inhibition**

Modification of chaperones to enable the manipulation of mutated proteins has been tested both in vitro and in vivo on model animal for therapeutic potential. The emphasis has been on chaperone Hsp90 because of easily accessible functional inhibitors of Hsp90 chaperone. Blocking the function of Hsp90 triggers the degradation of its 'specific protein', this provides basis of utility of these inhibitors in cancer to silence oncogenes in model animals. However the recognition of FGFR3 specificity to chaperone Hsp90 shows that signaling of FGFR3 is depended on Hsp90. So it need to determine whether Hsp90 inhibitors can block FGFR3 in achondroplasia. However there are few publications on influence of Hsp90 inhibitors on bone growth (Laederich and Horton., 2012).

#### **1.3.1.2.2.5 Other Therapeutic Approaches**

For ACH include growth hormone administration and a surgical procedures known as distraction osteogenesis (DO). While hormone treatment is useful in HCH but much less effective in ACH, as it may increase body size disproportionately and it is very costly. Additionally, DO is a very long and painful treatment that seriously affects the patient's quality of life. Currently DO has been combined with the transplantation of bone marrow-derived mesenchymal stem cells in an effort to decrease the treatment duration by accelerating bone formation (Martinez *et al.*, 2010).

#### **1.3.1.3 Hypochondroplasia**

Hypochondroplasia (HCH) is a autosomal dominant genetic disorder. General phenotypic characteristics of HCH similar to those of ACH, but in case of HCH phenotypic severity is less. Its characteristic features include shortening of the limbs, narrow spinal cord, short

fingers and shortened tubular bones. Both achondroplasia and hypochondroplasia are allelic, based on the similarities in their phenotype. HCH is caused by a C1620A/G mutation in FGFR3 gene, that result in Asn540Lys substitution in tyrosine kinase domain of FGFR3. Another mutation resulting in FGFR3 Ile538Val substitution is also confirmed in Italian hypochondroplasia patients (Vajo *et al.*, 2000).

#### **1.3.1.4 Thanatophoric dysplasia(TD)**

Thanatophoric dysplasia is more common neonatal lethal skeletal dysplasia with an incidence between 1/33,000 and 1/47,000 live births. It is characterized by shortening of limbs, macrocephaly, short stature with craniofacial abnormalities, narrow thorax, curved femur and flattened vertebral bodies. Thanatophoric is a Greek word which means “Death bearing”. It is an autosomal dominant disorder. Death of affected infants usually occurs because of respiratory failure and survival cases are rare (Horton., 2006). TD has been divided into two types on the basis of pattern of bone deformity.

##### **1.3.1.4.1. Thanatophoric dysplasia TypeI (TDI)**

Thanatophoric dysplasia Type I (TDI) is more common subtype and is characterized by curved femurs and humeri with a normal skull. This autosomal dominant disorder is caused by missense or stop codon mutations in extracellular or intracellular domains of FGFR3 gene. Almost 12 nonsense mutations have been yet discovered in the *FGFR3* gene which are involved in TDI. All these mutations added cysteine residue in extracellular domain of FGFR3 gene. The most common *FGFR3* gene mutation (c.742C>T), that leads to substitution of arginine by cysteine on 248 position of FGFR3 protein (R248C) in the extracellular domain of FGFR3 protein (Noe *et al.*, 2010).

##### **1.3.1.4.1 Thanatophoric dysplasia (TDII)**

Thanatophoric dysplasia Type II is less common and severe than TDI, characterized by relatively straight long bones and a clover leaf skull. TD II is caused by single mutation in FGFR3 gene (c.1948A>G), that leads to substitution of lysine by glutamic acid at 650 amino acid in tyrosine kinase 2 domain of FGFR3 protein (Noe *et al.*, 2010).

#### **1.3.1.5 SADDAN dysplasia**

SADDAN dysplasia was originally named SSB dysplasia, for skeletal, skin, and brain dysplasia because these three systems are affected in this condition. It is characterized by extreme short stature, unusual bowing of leg bones, acanthosis nigricans, a small chest with short ribs and curved collar bones, short and broad fingers, and folds of extra skin on

arms and legs and delay in development of intellectual and motor skills . A progressive skin disorder acanthosis nigricans develops in childhood , characterized by thick,dark and velvety skin. A novel mutation A1949T in the FGFR3 gene , leading to (Lys650Met) has been reported in patients with SADDAN dysplasia . Many of the features of SADDAN are similar to those seen in thanatophoric dysplasia but it differs in severity and like TD I it is not lethal (Tavormina *et al.*, 1999).

### **1.3.1.6.Craniosynostosis disorders**

FGFR3 gene mutations are not only involved in achondroplasia group disorders,however craniosynostosis skeletal disorder are also linked with mutations in FGFR3 gene.Two common craniosynostosis disorders are , Muenke coronal craniosynostosis and Crouzon syndrome with acanthosis nigricans.

#### **1.3.1.6.1Muenke coronal craniosynostosis**

Muenke coronal craniosynostosis autosomal dominant disorder, and characterized by radiographic abnormalities of hands and feet like, coned epiphysis ,fused carpal and tarsal, and thimble like middle phalanges. It is caused by C749G mutation in *FGFR3* gene that results in substitution of proline by arginine on 250 position of FGFR3 protein (Pro250Arg) in the extracellular domain.Considerable heterogeneity in phenotype has been observed in individuals with this disorder, as in some patients developmental delay, hearing loss and mental retardation has also observed (Bellus *et al.*, 1996; Muenke *et al.*, 1997).

#### **1.3.1.6.2 Crouzon syndrome with acanthosis nigricans.**

Crouzon syndrome is characterized by cloverleaf skull, hypertelorism, parrot- beaked nose, underdevelopment of maxillary bone, short upper lip, and dentofacial abnormalities. It is mainly caused by mutations in FGFR2 but recently a G1172A mutation has been identified in FGFR3gene that leads to substitution of Alanine by Glutamine (Ala391Glu) in the transmembrane domain of FGFR3 protein,recognized in individuals with phenotypes of Crouzon craniosynostosis in association with acanthosis nigricans. (Schweitzer *et al.*, 2001).

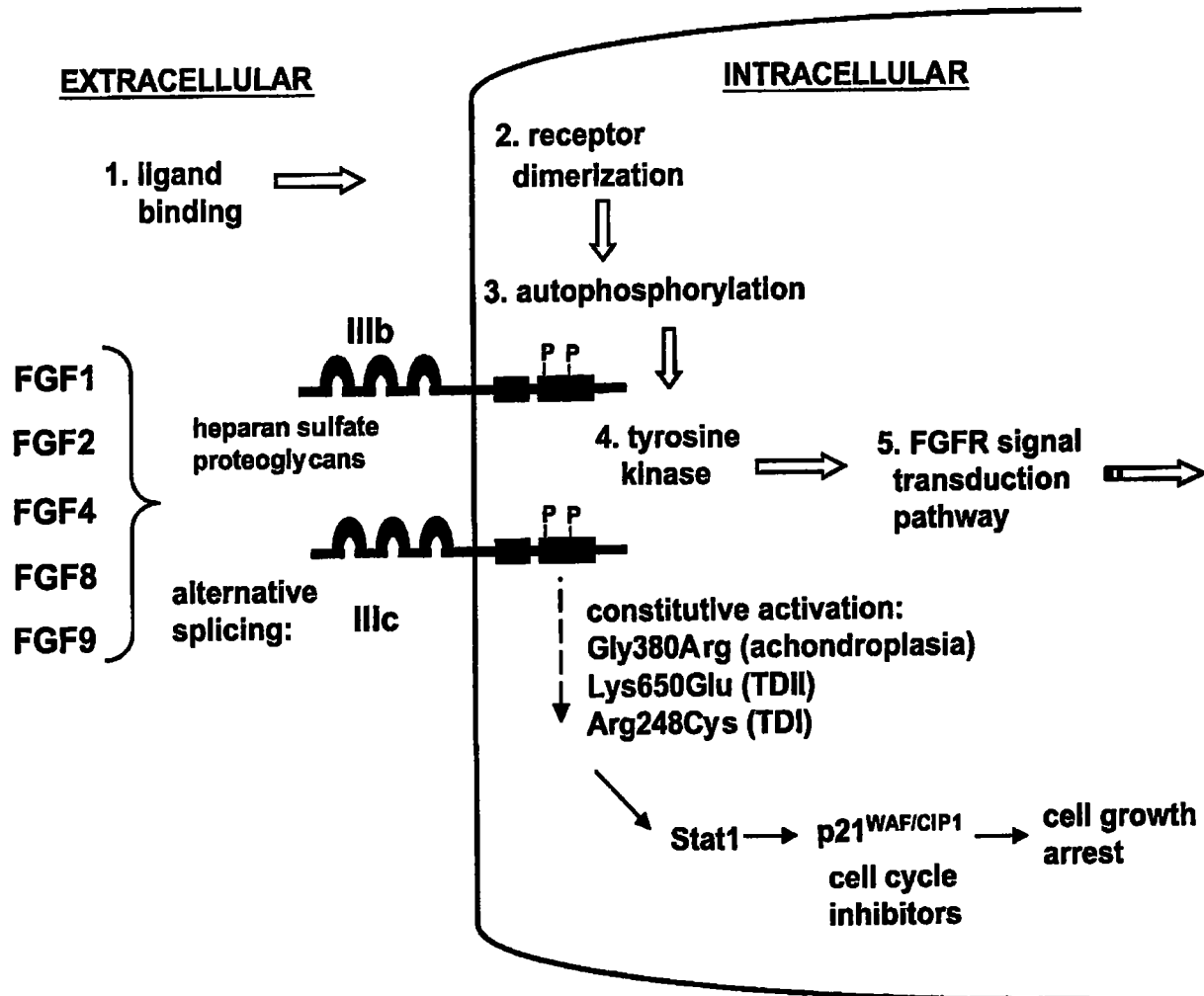


**FIGURE 1.1** A putative model for FGFR3 signaling. The receptor is shown with both a extracellular and intracellular domain. Binding of the ligand (FGF) to the receptor in the presence of heparan sulfate proteoglycans, results in receptor dimerization and autophosphorylation of several FGFR3 tyrosine residues in the cytoplasmic domain, which stimulates tyrosine kinase activity. These phosphorylated tyrosine residues provide a means to recruit and phosphorylate other molecules, furthering the FGFR3 signal transduction pathway. Recent studies have shown that mutations in the FGFR3 gene can allow constitutive, ligand-independent activation of the receptor. For the common achondroplasia and TD mutations, this leads to the activation of Stat1 and cell cycle inhibitors, eventually leading to cell growth arrest (Vjo *et al.*, 2000).

### 1.3.2 SCOLIOSIS

Scoliosis is a three dimensional deformity of vertebral column, consisting of lateral curvature spine and rotation of the vertebrae. Scoliosis may occur only in the thoracic area or lumbar region, but mainly occurs in the thoracolumbar area (between the thoracic and lumbar area). The severity of scoliosis depends on the extent of the spinal curvature and the angle of the vertebrae rotation.. In addition ,large scoliotic curve may cause pulmonary abnormalities, that in severe condition may lead to heart failure. (Trobisch *et al.*,2010)

#### 1.3.2.1 Classification of Scoliosis

Depending on underlying cause, scoliosis can be classified broadly as, **Congenital, Neuromuscular, Syndrome-related and Idiopathic scoliosis** (Janicki and Alman ,2007).

##### 1.3.2.1.1 Congenital

It is due to inborn vertebral deformities, that usually involve abnormalities in formation and development of vertebra (absent or fused vertebrae), the condition become evident as curvature of spine (Giampietro.,2012).

##### 1.3.2.1.2 Neuromuscular

In this case scoliosis may develop as secondary to neuromuscular/neurological disease such as cerebral palsy, Duchenne's muscular dystrophy, Friedreich ataxia ,and spinal muscular atrophy (Janicki and Alman.,2007).

##### 1.3.2.1.3 Syndrome-related

This type of scoliosis occurs along with syndromes, like Marfan syndrome and Ehlers-Danlos syndromes .

##### 1.3.2.1.4 Idiopathic Scoliosis

Idiopathic scoliosis is a malformation of spine of unknown etiology, characterized by spinal curvature and vertebrae rotation (Good.,2009).

###### 1.3.2.1.4.1 Classification of Idiopathic Scoliosis

Idiopathic scoliosis is categorized on the basis of patient's age at the time of disease onset:

- infantile Idiopathic scoliosis (Birth to age 3),

- juvenile Idiopathic scoliosis (ages 3 to 9), and
- adolescent Idiopathic scoliosis (ages 10 to 18).

**Infantile curves** may be associated with, asymmetrical distortion of the skull, hip dysplasia, heart disease and neuroaxial abnormalities, and usually 80% cases resolve itself spontaneously and need no treatment. On the other hand, **Juvenile scoliosis** effects the body during developmental years so it has ability to deform trunk leading to severe cardiac or respiratory problems. If left untreated, curves that reach 30° are almost always progressive (Trobisch *et al.*,2010)

Scoliosis is often categorized on the basis of shape of the curve, either structural or nonstructural.

#### **1.3.2.1.5Nonstructural scoliosis**

Nonstructural (functional) scoliosis involves a side to side spine curve ,without twist,it is caused by poor posture, muscle spasm and difference in leg length.

#### **1.3.2.1.6 Structural scoliosis**

Structural scoliosis characterized by a curved spine, with rotation of spine and is usually caused by an unknown factor (idiopathic) or a disease or syndrome.

#### **1.3.2.2 Adolescent idiopathic scoliosis (AIS)**

Adolescent idiopathic scoliosis (AIS) is a complex spinal abnormality along with axial rotation ,of unknown cause and characterized by lateral curvature  $>10^\circ$   
(Czeizel *et al.* ,1978)

#### **1.3.2.2.1 Prevalence**

Idiopathic form of scoliosis is less common in infants and in childhood, its occurrence in children up to age 15 of about 1% to 2%. And its prevalence is 8% in adults of 25age , incidence rate rises to almost 68% in 60 to 90 aged persons. The probability of adolescent scoliosis progression depends on Cobb angle, if a Cobb angle is in range of 20° then probability of progression becomes 10% to 20%. However Cobb angle greater than 20° along with under developed bones in adolescents , the probability of progression become 70% or greater (Edery *et al.*,2011).

### 1.3.2.2.2 Symptoms

AIS is usually painless deformity. Adolescent idiopathic scoliosis characterize by disproportionate shoulder (one shoulder elevated than other) uneven waist line, hips asymmetry and difference in limbs size., although there is no movement problem in AIS (Wise *et al*., 2008).

### 1.3.2.2.3. Diagnosis of AIS

AIS is diagnosed on the basis of physical examination and radiographic criteria. Accurate diagnosis requires the whole vertebral column X-ray of patient with standing posture. However shoulder symmetry can be observed by taking in account the clavicles and iliac crests . The severity of scoliosis is determined by measuring the Cobb angle. Cobb angle can be determined by observing the tilting of two vertebral bodies from horizontal axis . A Cobb angle of greater than  $10^\circ$  is identified as diseased, but it is considered scoliosis only when rotational deviation is also observed (Ocaka *et al.*,2007).

### 1.3.2.2.4. Treatment of AIS

Adolescent idiopathic scoliosis can be treated by taking in account characteristics like age of patient , severity and position of the curve. Treatment includes:

- Observation,
- Bracing,
- Surgery

Patients with mild curves that is between 0-20 degrees are observed periodically on a 4 to 6 month basis .Patients radiographs are taken to observe extent of curve progression. However patients with risk for progression and large size curves almost 20 to 40 degrees and that are at during rapid growth phase are treated with brace. Purpose of bracing is not to treat the curve but to inhibit curve progression. The beneficial effects of a bracing is based on maximum duration the patient wears the brace. The brace is recommended to be worn between 16 and 23 hours a day and continued to use until growth has completed. Surgery is usually indicated for curves greater than  $40^\circ$  in a AIS patients and for curves that progress despite bracing. The main purpose of surgery is to not only prevent curve progression but also to correct the spinal curvature. Depending on curve nature, curve flexibility and position of curve, surgical treatment of scoliosis can be used in many ways

(Adobor *et al.*, 2014).

### 1.3.2.2.5 Idiopathic Scoliosis related Genes

Involvement of genetic and environmental factors in idiopathic scoliosis have been identified by various techniques. The candidate genes for idiopathic scoliosis have been identified in model animals. These genes play role in various stages of spinal development, however the number of candidate genes will continue to increase. Allelic mutations in candidate genes may be cause of the idiopathic scoliosis. Advancement in research will be helpful to recognize the candidate genes involved in these disorders. These candidate genes are identified in signaling pathways, intracellular signal transduction, encodes various matrix proteins, and involved in matrix metabolism (Shangguan *et al.*, 2008). However for the several years, the contribution of candidate genes in the development of idiopathic scoliosis have been extensively studied.

#### SNTG1 (Gamma-1-syntrophin)

Investigation of mutations in exons of SNTG1 gene in 152 idiopathic scoliosis patients have shown a 6-bp deletion in exon 10 in one patient and a 2-bp insertion/deletion in two patients (Giampietro *et al.*, 2003). However these mutations has not been identified in 480 control chromosomes. Thus, SNTG1 gene plays role in maintenance of posture and contribute towards development of idiopathic scoliosis (Wise *et al.*, 2008).

#### Aggrecan

Aggrecan is a proteoglycan constituent of disc matrix. The inadequate production of aggrecan in growth plate of vertebrae, leads to development of idiopathic scoliosis. This shows that malfunction of aggrecan gene, may be one of the cause of idiopathic scoliosis (Gorman *et al.*, 2012).

#### CHD7 (Chromodomain-helicase-DNA-binding gene 7)

Genome wide scans of 52 families was conducted, and identified that CHD7 gene polymorphisms are involved in idiopathic scoliosis. The possible SNP loci are contained within a 116-kb region of CHD7 gene. Since girls are mainly affected by idiopathic scoliosis, the association between polymorphism of estrogen receptor gene and severity of idiopathic scoliosis was identified and revealed the average Cobb's angle of genotype XX and Xx is

bigger than the *xx* genotype also the risk of operation is higher. Few studies proposed that malfunction of *CHD7* gene in the postnatal period, mainly in adolescent, may disturb normal skeletal development and contributes to spinal abnormality (Wise *et al.*, 2008).

## **MESP1 AND MESP2**

Both *MesP1* and *MesP2* are helix-loop-helix transcription factors. Studies conducted in zebrafish have showed that interaction of these genes with the fibroblast growth factor receptor is important in establishment of the anterior-posterior polarity of growing somite (Shangguan *et al.*, 2008).

### **Pax1 (Paired box gene 1)**

*Pax1* is localized on 20p11. *Pax1* plays role in differentiation of sclerotome, so its dysfunction results in vertebral abnormalities. Mutation analysis of *Pax1* gene has revealed mutations in three alleles in model mouse. However mutations in these alleles result in decrease or inhibition of *Pax1* gene expression, that ultimately leads to under development of the anterior vertebral element (Gorman *et al.*, 2012).

### **BMP-7 (Bone morphogenic gene 7)**

Bone morphogenic protein are component of bone matrix, and represents transforming growth factor- $\beta$ . Mice carrying both mutant BMP-7 allele shows skeletal abnormalities, like lack of lumbar vertebrae and absence of union of neural spines of the atlas, twelfth thoracic and first sacral vertebrae. Mutant mice lacks ossification centers. So the BMP-7 protein plays important role in ossification process (Gorman *et al.*, 2012).

### **Ky (kyphoscoliosis peptidase)**

The *Ky* gene encodes a novel muscle specific protein, localized on chromosome 9. A deletion mutation has been identified *ky/ky* mice that results in premature stop codon at position 125. Myosin light polypeptide kinase is situated in this region so it may be a candidate gene for idiopathic scoliosis (Shangguan *et al.*, 2008).

### **LMX1A (homeobox transcription factor 1, alpha)**

*Lmx1a* serves a role in differentiation of cells in the central nervous system and in

developing vertebrae. Lmx1a maps to a region, 1q22-q23 and are immediate structures during early central nervous system development (Wise *et al.*, 2008).

### **SIM2 (Single-minded homolog 2)**

Sim2 related to a family of transcription factors, located on human chromosome 21q22.2, characterized by a basic helix-loop-helix-domain, that is similar to 67.6 region of mouse chromosome 16. Malfunction of Sim2 in mice leads to development of idiopathic scoliosis characterized by uneven vertebrae and ribs, as a result death of mice occurs readily after birth because of respiratory failure. Sim2 have role in later stages of vertebral development, because Sim 2 expresses in vertebral body not in somites. So it is postulated that excessive growth of ribs in Sim2 dysfunction mice is a cause of idiopathic scoliosis (Gorman *et al.*, 2012).

### **BPTF (bromodomain PHD finger transcription factor)**

The bromodomain motif of BPTF is highly conserved, have role in protein protein interaction. BPTF plays an important role in development of vertebrae during early ontogenesis. Malfunction of BPTF during adolescent, along with other factors could lead to development of idiopathic scoliosis (Shangguan *et al.*, 2008).

### **MATN1( Matrilin 1, cartilage matrix protein)**

MATN1 is largely expressed in cartilage and is located at 1p35. The linkage analysis was conducted on sample of 81 trios, as a result linkage disequilibrium was identified among the matrilin-1 (MATN1) gene and idiopathic scoliosis. Each trios consist of both parents and their daughter/son, all were affected of idiopathic scoliosis. In all trios, amplification of a specific microsatellite marker possessing region of MATN1 gene was carried out by polymerase chain reaction. In this way, three polymorphisms 103 bp, 101 bp and 99 bp, were observed, while the transmission of only 103bp allele become evident. Thus, MATN1 gene involve in the idiopathic scoliosis (Gorman *et al.*, 2012).

## 1.4 OBJECTIVES

Skeletal dysplasia are group of complex disorders and full understanding has not yet been developed, due to involvement of multiple factors and heterogeneous nature of disorders. Clinical presentation of patients with small differences in different patients can mislead in diagnosis of accurate phenotype .So it will be useful to go for genetic study. The aim of study was to gain knowledge about genetic mechanism involved in development of skeletal disorders. The main objectives of study are:

1. To identify the loci involved in Inherited Skeletal Dysplasia in Pakistani population by linkage analysis.
2. Screen out the genes for the identification of any sequence variants in affected members.

# **CHAPTER 2**

# **MATERIALS AND**

# **METHODS**

## Materials and Methods

### 2.1 Study subject

The aim of present study was to identify the gene/ loci involved in Inherited Skeletal Dysplasia. Two Pakistani families (A and B) having symptoms of skeletal disorders were located and sampled for this purpose. The study was commenced after getting the approval from Ethical and Review committee of International Islamic University Islamabad, Pakistan.

### 2.2 Families History and Analysis

Blood specimens and related information of both Families were obtained by visiting at their homes. Skeletal deformities and other abnormalities of affected individuals were noted and analyzed. Information like number of affected individuals and family history was obtained. Parents signed the consent form and had no objection in terms of blood acquisition and publishing of photographs of the affected individuals.

### 2.3 Pedigree Construction and Interpretation

Based on the information obtained from guardians like number of affected and normal individuals and existence of consanguinity, pedigrees were drawn by the method described by (Bennett *et al.*, 2008). Generation numbers indicated by Roman numerals and individuals within a generation were represented by Arabic numerals. The individual numbers labeled with asterisks indicated the samples collected for this study. In a pedigree affected female and males were indicated by filled circles and squares, respectively. Crossed symbols represented the deceased individuals. Double lines between individuals showed consanguineous marriage.

### 2.4 Blood Acquisition

Blood samples of all available both affected and normal individuals were obtained through 10 ml sterilized syringes by venous route. Blood samples were transferred to the vacutainer having ethylenediaminetetraacetic acid (BD Vacutainer® K3 EDTA, Franklin Lakes NJ, USA) and stored at 4°C. (Puri *et al.*, 2009).

## 2.5 EXTRACTION OF GENOMIC DNA

Genomic DNA from blood samples was extracted by the standard Phenol-Chloroform method.

### 2.5.1 Phenol-Chloroform method.

Using standard Phenol-Chloroform method, genomic DNA from blood samples was extracted by following protocol. . To 5 ml whole blood sample (EDTA, heparin, citrate) three volumes of RBC lysis buffer ( 15 ml ) was added, shaked gently, mixed by vortexing , incubated for 30 min on ice, and centrifuged at 1200 rpm for 10 min at 4°C. Supernatant was removed, resuspend the pellet by adding 10 ml lysis buffer and centrifuged at 1200 rpm(4°C) for 15min. Again supernatant removed , resuspend the pellet by adding 5 ml STE-buffer , vortexed and dropwise 250  $\mu$ l 10% SDS added .Finally 10 $\mu$ l proteinase K (10mg/ml) added and incubated overnight at 55°C in a water bath .

Next day ,equal volume of phenol added (equilibrated with Tris, pH 8) to the tube and mixed by inverting, ,incubated for 10 min on ice . The tube was centrifuged at 3200 rpm for 40 min at 4°C. Aqueous layer was separated, transferred into a new tube, then equal volume of chloroform:isoamyl alcohol( 5 ml) added , gently shaked, incubated on ice for 10 min, and centrifuged at 3200 rpm for 40 min at 4°C. Supernatant was separated and transferred into a new tube, 200  $\mu$ l sodium acetate (pH 5.2) and 5 ml isopropanol was added, gently shaked until pellet visualized, that was the precipitated DNA. Now stored that aqueous layer containing pellet at -20 °C overnight.

Next day centrifugation was carried out at 3200 *rpm* at (4°C) for 50 min. The supernatant was discarded, and resuspended in 5ml 70% ethanol, and the pellet was tapped gently, followed by centrifugation at 3200 rpm for 40 min at 4 °C, supernatant gently decanted. The pellet was airdried overnight, and the dried pellet was resuspended in 300  $\mu$ l 1× TE buffer and frozen at -20°C or -80°C for storage. Composition of solutions given in table 2.1 (Sambrook *et al.*, 1989).

**Table 2.1 Composition of solutions**

Solutions	Composition	Purpose
<b>Cell -Lysis buffer</b>	KHCO <sub>3</sub> 1gm/L NH <sub>4</sub> CL 8.29gm/L 0.5M EDTA 0.34gm	Cell lysis buffer cleaves the cell membrane and exposes chromatin material of nucleated cells.
<b>STE Buffer</b>	3M NaCl 33.3ml 1M Tris-HCl 4.0ml 0.5M EDTA 2.0 ml	STE buffer provides saline environment to newly exposed chromatin material.
<b>DNA Dissolving Buffer</b>	10mM Tris-HCl 0.1mM EDTA	This buffer is used for dissolving the DNA.
<b>10%SDS</b>	SDS 10g Distilled water 50ml	10%SDS helps in protein degradation.
<b>Chloroform-Isoamyl Alcohol</b>	Chloroform 480ml Isoamyl alcohol 20ml	It is used to separate protein and polysaccharides from DNA.

## 2.6. DNA CONCENTRATION AND PURITY DETERMINATION

A quantitative spectrophotometric analysis of DNA was performed using a Nano drop spectrophotometer. The Nano Drop ND-1000 spectrophotometer uses a patented system that holds ~1  $\mu$ l of sample without the need for traditional containment devices such as cuvettes and capillaries. Absorbance was measured at wavelengths of 260 and 280nm ( $A_{260}$  and  $A_{280}$ , respectively). The absorbance quotient ( $OD_{260}/OD_{280}$ ) provides an estimate of DNA purity. An absorbance quotient value of  $1.8 < \text{ratio (R)} < 2.0$  was considered to be good, purified DNA. A ratio of  $<1.8$  is indicative of protein contamination, whereas a ratio of  $>2.0$  indicates RNA contamination.

## 2.7 DNA INTEGRITY

The genomic DNA integrity was determined by analyzing DNA samples on a 1% agarose gel by melting 0.5 g of agarose in 50ml 1X TBE in microwave oven for 1-2 minutes. 5  $\mu$ l ethidium bromide was added to gel to stain the DNA. The DNA was mixed with loading dye and loaded into wells of agarose gel. The electrophoresis was performed at 120 volts for 30 minutes then visualized under UV trans illuminator and results were recorded by using gel documentation.

## 2.8 POLYMERASE CHAIN REACTION

Genomic DNA was diluted to 40-50 ng/ $\mu$ l for Polymerase chain reaction (PCR).. A 25  $\mu$ l reaction mixture was taken in a 0.5 ml reaction tube containing 2.5  $\mu$ l of 10 X  $(NH_4)_2SO_4$  buffer , 1.5  $\mu$ l (1 mM)  $MgCl_2$ , 0.3  $\mu$ l of each primer, 0.5  $\mu$ l (0.2 mM) of dNTP mix, 1  $\mu$ l of diluted genomic DNA (40-50 ng/ $\mu$ l), 0.2  $\mu$ l of Taq DNA polymerase and 18.7  $\mu$ l of PCR water. The reaction mixture was centrifuged for few seconds to mix it thoroughly. The standard thermal cycle conditions used included one cycle of denaturation at 96°C for 5 minutes, followed by 40 cycles of amplification each consisting of 3 steps: denaturation of DNA into single strand at 95°C for one minute, annealing or hybridization of microsatellite markers to their complementary sequences on either sides of target sequence at 50-60°C for one minute, and final extension for 10 minutes at 72°C. The extension step included initial denaturation cycle for one minute at 95°C, 48 cycles with 30 seconds denaturation at 95°C, 30 seconds annealing with progressively lowering temperature from 70 to 53°C at a rate of 1°C every third cycle and a primer extension of

40 seconds at 72°C, followed by 15 additional cycles with an annealing temperature of 58°C and final extension at 72°C for ten minutes (Frey *et al.*, 2008)

## 2.9 LINKAGE ANALYSIS

The families included in this research work were subjected to linkage analysis. Highly polymorphic microsatellite markers (average heterozygosity > 75%) flanking the known genes loci involved in hereditary skeletal dysplasia were used. Microsatellite markers used for linkage analysis are given in Table 2.2 and 2.3.

## 2.10 GEL ELECTROPHORESIS

### 2.10.1 POLYACRYLAMIDE GEL ELECTROPHORESIS (PAGE)

8% non-denaturing polyacrylamide gel was used for the resolution of amplified PCR products. The gel was prepared by mixing 13.5ml of 30% acrylamide solution, , 5ml 10 X Tris-Borate-EDTA (Tris0.89 M, Borate 0.89 M, EDTA 0.02 M), 350  $\mu$ l 10% APS (Ammonium persulphate) , 25  $\mu$ l TEMED (N, N, N', N'-Tetra methylethylene diamine) and 50 ml distilled water in a beaker . The gel solution was poured between two cleaned glass plates held apart by a spacers of 1.5 mm thickness. A comb was inserted from top in the gel and allowed to dry for half an hour .The PCR DNA product was mixed with 5 $\mu$ l bromophenol blue dye (0.25% bromophenol blue in 40% sucrose solution) and then electrophoresis was performed at 100 volts for almost 3 hours in vertical gel electrophoresis apparatus (Whatman, Biometra, Gottingen, Germany) ,that was inserted in 1X Tris-Borate-EDTA buffer. The gel was dipped in ethidium bromide (10  $\mu$ g/ml) solution for staining , and visualized on UV trans illuminator (Biometra, Gottingen, Germany). The gel photograph was taken by using electrophoresis analysis system DC 290 (Kodak, Digital Sciences, New York, USA).

**Table 2.2** List of microsatellite markers used to test linkage to genes involved in Achondroplasia.

S. NO	Gene	Chromosome	Markers	cM
1	<b>FGFR3</b> <b>Fibroblast Growth Factor Receptor3</b>	4p16.3	D4S2936	0.61
			D4S43	2.86
			D4S127	3.6
			D4S179	3.99
			D4S2957	5.72
			D4S3023	6.54
			D4S2925	7.17
			D4S394	14.94
2	<b>NPR2</b> <b>Natriuretic Peptide Receptor B</b>	9p21-p12	D9S1678	54.78
			D9S319	55.51
			D9S1118	57.01
			D9S1817	59
			D9S1874	61.38
			D9S55	62
			D9S773	64.28
			D9S1110	69
3	<b>MaP2K1</b> <b>Mitogen Activated Protein Kinase 1</b>	9 C	D9S50	60.81
			D9S229	62.66
			D9S1879	66.89
			D9S15	67.37
			D9S1806	69.4
4	<b>NPPC</b> <b>Natriuretic peptide C</b>	2q37.1	D2S2213	236.47
			D2S396	237.40
			D2S2317	237.74
			D2S427	240.12
			D2S2344	241.10

**Table 2.3** List of microsatellite markers used to test linkage to loci involved Adolescent Idiopathic Scoliosis (AIS).

Locus	Chromosomal Location	Markers	cM
IS1	19p13.3	D19S894	13.95
		D19S1034	18.21
		D19S567	22.98
		D19S884	23.69
		D19S916	27.33
		D19S865	28.23
		D19S221	32.91
IS2	17p11.2	D17S839	41.92
		D17S1856	39.76
		D17S1843	45.95
		D17S2196	47.28
		D17S842	49.4
		D17S783	50.54
		D17S1878	51.2
		D17S1800	53.14
IS3	8q12	D8S1471	122.32
		D8S565	123.01
		D8S592	124.85
		D8S527	125.12
		D8S199	126.4
IS4	9q31.2-34.2	D9S1105	119
		D9S1776	123.79
		D9S1685	132.42
		D9S291	139
		D9S766	142
		D9S1793	149.91
IS5	17q25.3-qter	D17S1847	122
		D17S1806	125
		D17S784	127.8
		D17S914	131.07
		D17S668	133.61

# **CHAPTER 3**

# **RESULTS**

## RESULTS

### 3.1 FAMILY A

Family A with autosomal recessive achondroplasia, was collected from Islamabad. This is a four generation pedigree. Five members of the family A were available for blood sampling. These include three affected individuals, two males (IV-1, IV-2) and one female (IV-4). One of the affected male individual had deceased as illustrated in figure 3.1. All three affected individuals showed achondroplasia (MIM: 100800). No other abnormality was found in the affected individuals (Fig.3.2 a and b). Pedigree analysis revealed that parents and one sibling of affected individuals were normal, also the individuals were affected irrespective of their sex suggesting that in this family achondroplasia is inherited in autosomal recessive mode. Blood samples of two affected and three normal individuals were collected for the present study.

### 3.2 FAMILY B

Family B resides in district Sawabi, Khyber Pukhtunkhwa Pakistan. The pedigree was constructed after careful investigations with family elders to avoid any error. The parents of affected individuals are cousins to each other. This is a four generation pedigree. Ten members of the family B were available for blood sampling. These include three affected individuals, out of them two were male (IV-1, IV-2) and one was female (IV-6) as illustrated in figure 3.3. Affected individuals exhibit Adolescent Idiopathic Scoliosis (MIM: 181800), characterized by curved spine, shoulders asymmetry and uneven hips with no other complications (Fig.3.4 a,b and c). Pedigree analysis revealed that parents and three siblings of affected individuals were normal, which suggest that in this family Adolescent Idiopathic Scoliosis has autosomal recessive mode of inheritance. Blood samples of three affected and seven normal individuals were collected for the present study.

### 3.3 Mapping of genes/loci involved in Achondroplasia

Genetic linkage analysis was performed to check the linkage in particular family with known gene and loci involved in achondroplasia. Family A was tested for genetic linkage of four known genes including, FGFR3, NPR2, MaP2K1 and NPPC. Highly polymorphic microsatellite markers were used for investigation of linkage of family A with known genes. Using standard PCR reaction and polyacrylamide gel electrophoresis, genotyping analysis was carried out as discussed in materials and method section. Amplified PCR products were visualized after staining the gel with ethidium bromide and genotypes were assigned by visual

inspection. The particular family is considered linked to the respective gene, if homozygous banding pattern for mutant allele was observed for affected individuals, heterozygous banding pattern in carriers, and homozygous banding pattern for wild type allele in normal individuals, whereas the corresponding family is considered as excluded, if heterozygous banding pattern for mutant allele is shown in affected individuals. In family A five DNA samples, including three normal (III-7, III-8, IV-3) and two affected (IV-1, IV-4) were subjected for genotyping.. Analysis of results showed that the family A was not linked to any of four genes checked for linkage, as illustrated in figures 3.5-3.31. This suggests the involvement of a novel gene yet to be discovered as responsible for achondroplasia in this family.

### **3.4 Mapping of Genes/loci Involved in Adolescent Idiopathic Scoliosis**

Genetic linkage analysis was performed to check the linkage in particular family with known gene and loci involved in Adolescent idiopathic scoliosis. Family B was tested for genetic linkage of five known loci including, IS1, IS2, IS3, IS4 and IS5. Using standard PCR reaction and polyacrylamide gel electrophoresis, genotyping analysis was carried out by using highly Polymorphic microsatellite markers. In family B, DNA sample of five normal individuals (III-3, III-4, IV-3, IV-4, IV-5) and three affected individuals (IV-1, IV-2, IV-6) were tested for linkage by typing microsatellite markers for respective loci. Analysis of results showed that the family B was not linked to any of five loci checked for linkage, as illustrated in figures 3.32- 3.62. This suggests the involvement of a novel gene yet to be discovered as responsible for Adolescent idiopathic scoliosis in this family.

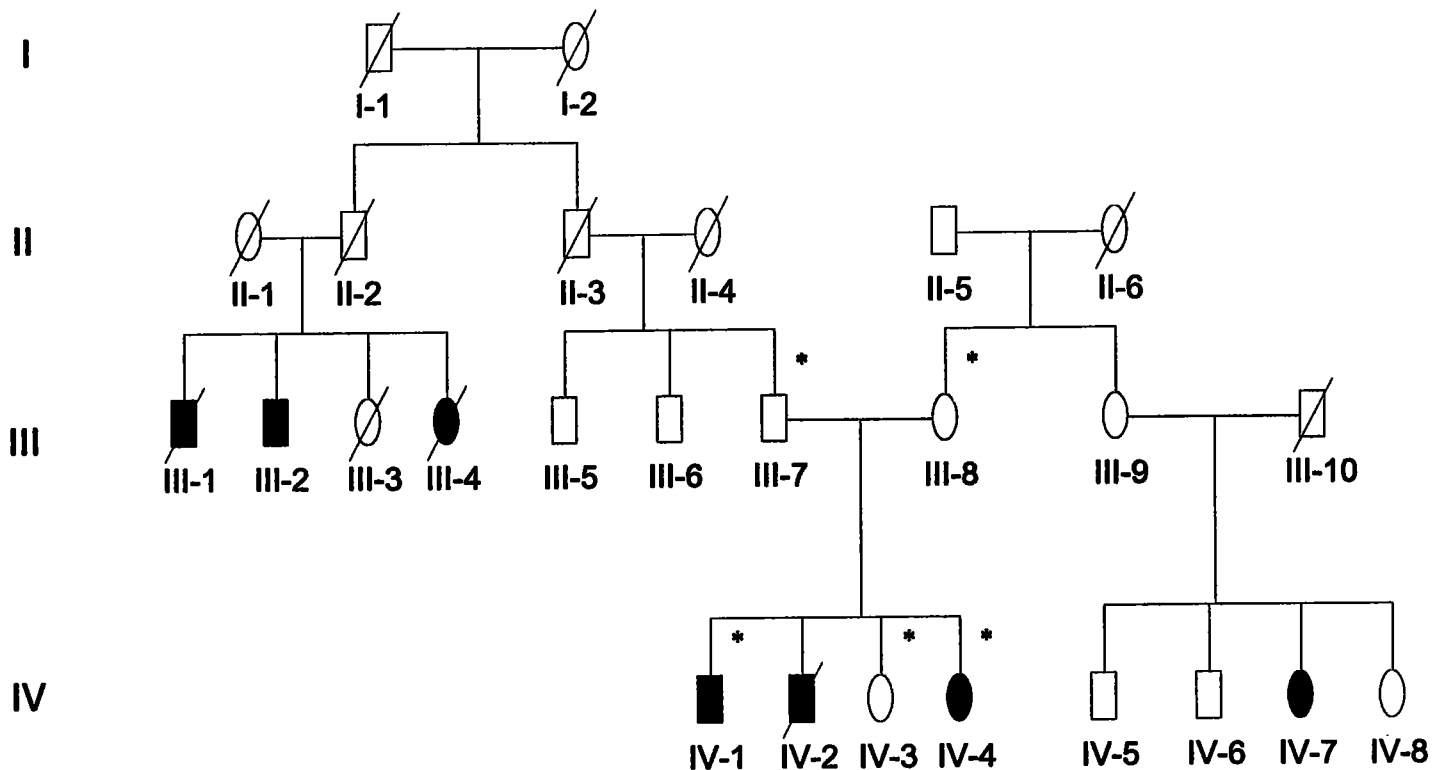


**Figure 3.1** Pedigree drawing of the family A segregating autosomal recessive achondroplasias. Affected males and females are indicated by filled squares and circles, respectively. Crossed symbols indicate the deceased individuals. The individual numbers labeled with asterisks indicate the samples available for this study



**Figure 3.2 (a).** An affected individual (IV-1) of family A, showing characteristic features of Achondroplasia, short limb dwarfism, frontal bossing, macrocephaly and depressed nasal bridge.



**Figure 3.2(b).** An affected individual (IV-4) of family A, showing characteristic features of Achondroplasia, bowed legs, disproportionate short stature and protruding chest.

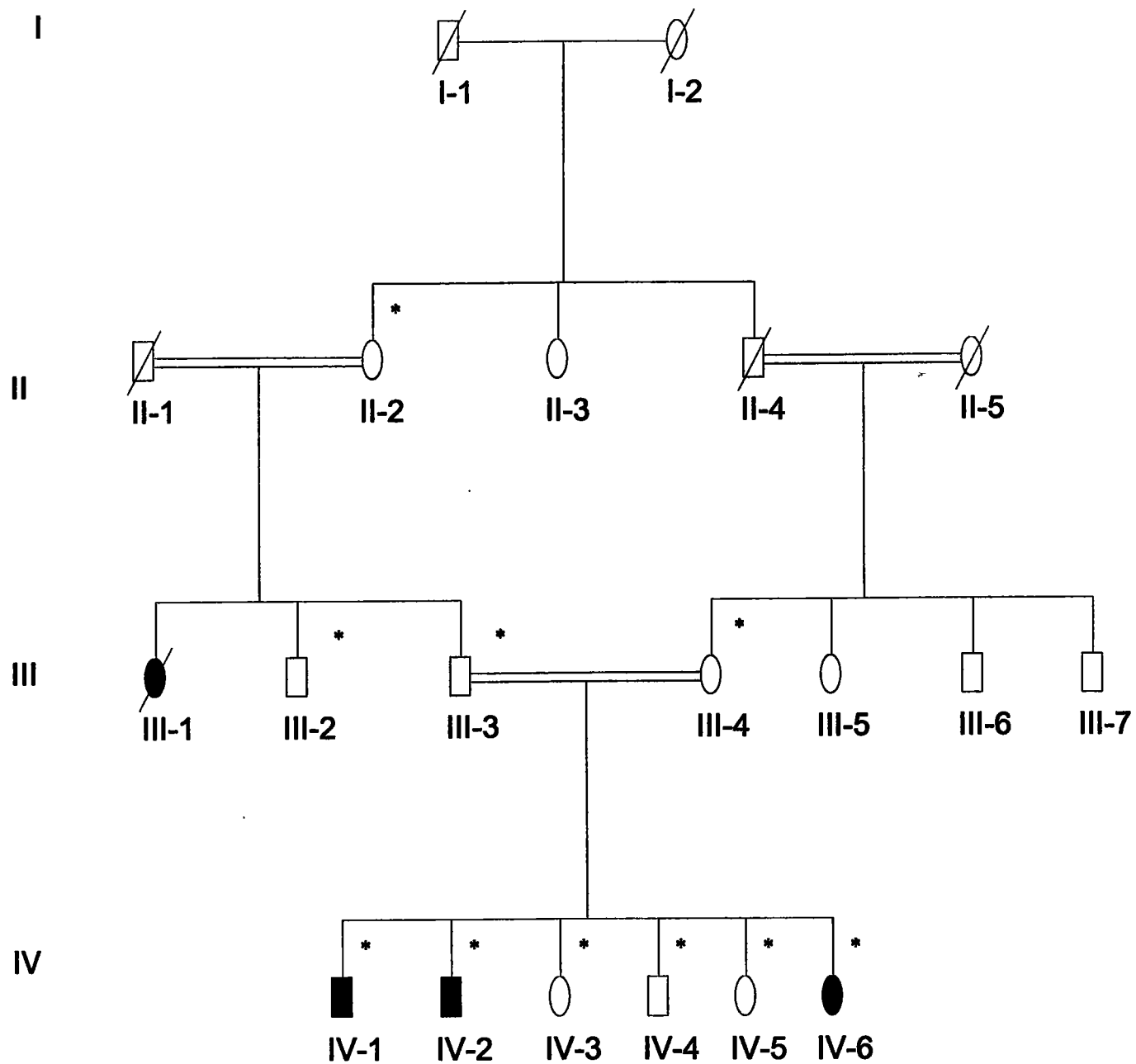


**Figure 3.3** Pedigree drawing of the family B segregating autosomal recessive Idiopathic Scoliosis. Affected males and females are indicated by filled squares and circles, respectively. Crossed symbols indicate the deceased individuals. Double lines between individuals represent consanguineous union. The individual numbers labeled with asterisks indicate the samples available for this study



**Figure 3.4 (a).** An affected individual of AIS (IV-1) of family B, showing characteristic features of adolescent idiopathic scoliosis, spinal deformity, lateral curvature, disproportionate shoulder and uneven hips.

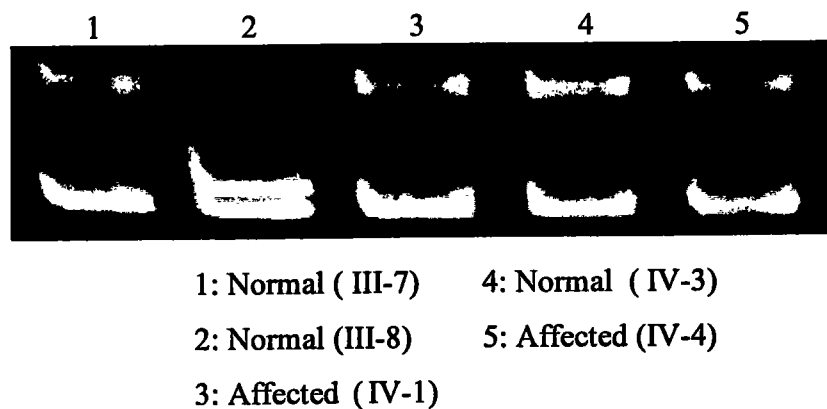
74-16124



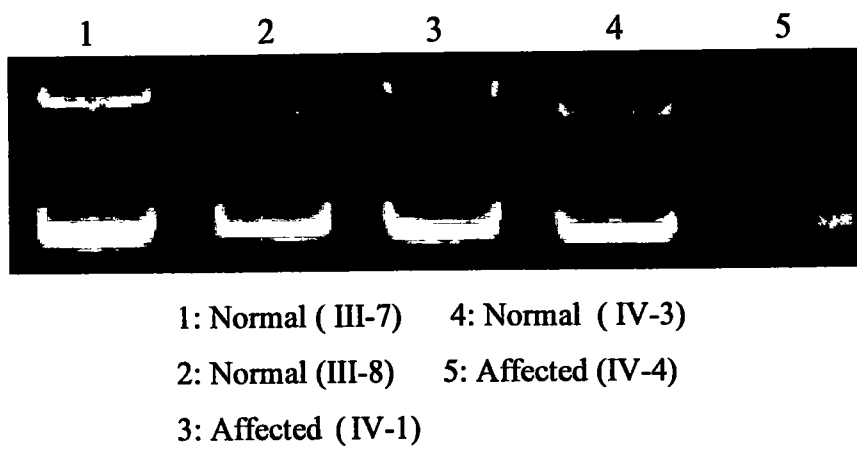
**Figure 3.4: (b).** An affected individual of AIS (IV-2) of family B showing characteristic features of adolescent idiopathic scoliosis, spinal deformity, lateral curvature, disproportionate shoulder and trunk asymmetry.



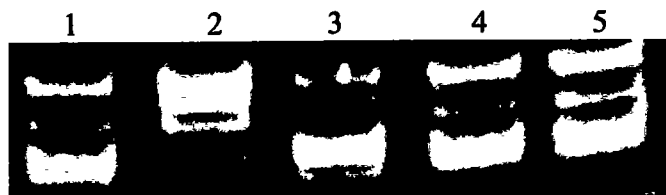
**Figure 3.4 (c).** An affected individual of AIS (IV-6) of family B:

**Family A: FGFR 3(4p16.3)**

**Figure 3.5:** Electropherogram of ethidium bromide stained 8% non-denaturing polyacrylamide gel for marker D4S2936 at 0.61 cM on chromosome 4p16.3. The Roman numerals indicate the generation number of the individuals within pedigree while Arabic numerals indicate their positions within a generation.

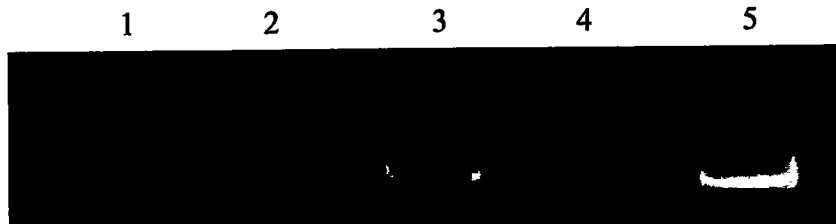
**Family A**

**Figure 3.6:** Electropherogram of ethidium bromide stained 8% non-denaturing polyacrylamide gel for marker D4S43 at 2.86 cM on chromosome 4p16.3. The Roman numerals indicate the generation number of the individuals within pedigree while Arabic numerals indicate their positions within a generation.

**Family A**

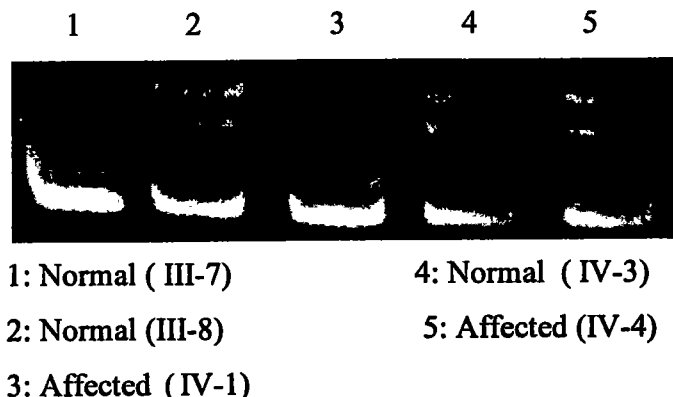
1: Normal ( III-7)      4: Normal ( IV-3)  
2: Normal (III-8)    5: Affected (IV-4)  
3: Affected (IV-1)

**Figure 3.7:** Electropherogram of ethidium bromide stained 8% non-denaturing polyacrylamide gel for marker D4S127 at 3.6 cM on chromosome 4p16.3. The Roman numerals indicate the generation number of the individuals within pedigree while Arabic numerals indicate their positions within a generation.

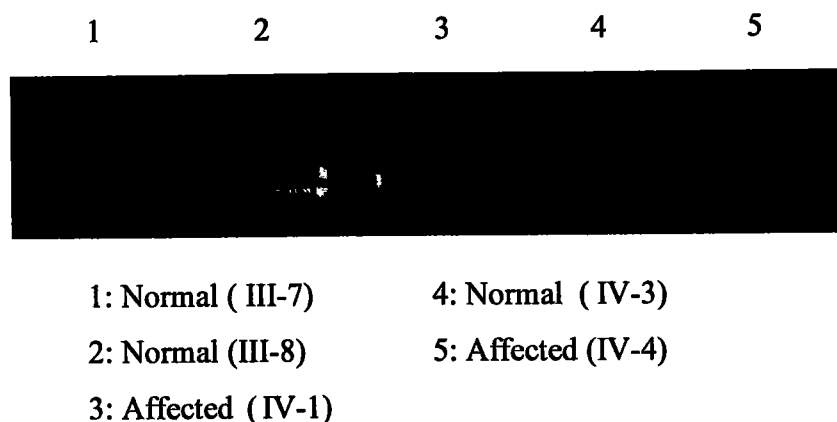
**Family A**

1: Normal ( III-7)      4: Normal ( IV-3)  
2: Normal (III-8)    5: Affected (IV-4)  
3: Affected (IV-1)

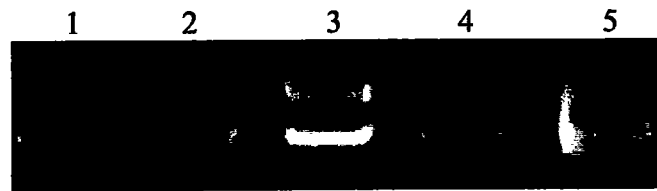
**Figure 3.8:** Electropherogram of ethidium bromide stained 8% non-denaturing polyacrylamide gel for marker D4S179 at 3.99 cM on chromosome 4p16.3. The Roman numerals indicate the generation number of the individuals within pedigree while Arabic numerals indicate their positions within a generation.

**Family A**

**Figure 3.9:** Electropherogram of ethidium bromide stained 8% non-denaturing polyacrylamide gel for marker D4S2957 at 5.72 cM on chromosome 4p16.3. The Roman numerals indicate the generation number of the individuals within pedigree while Arabic numerals indicate their positions within a generation.

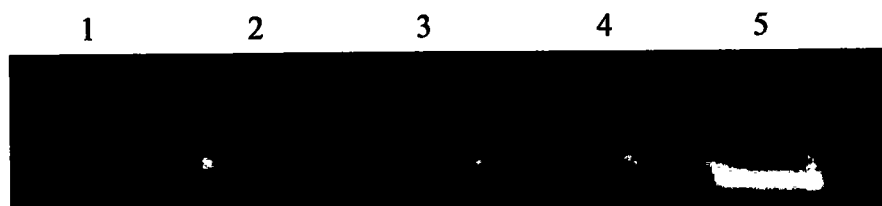
**Family A**

**Figure 3.10:** Electropherogram of ethidium bromide stained 8% non-denaturing polyacrylamide gel for marker D4S3023 at 6.54 cM on chromosome 4p16.3. The Roman numerals indicate the generation number of the individuals within pedigree while Arabic numerals indicate their positions within a generation.

**Family A**

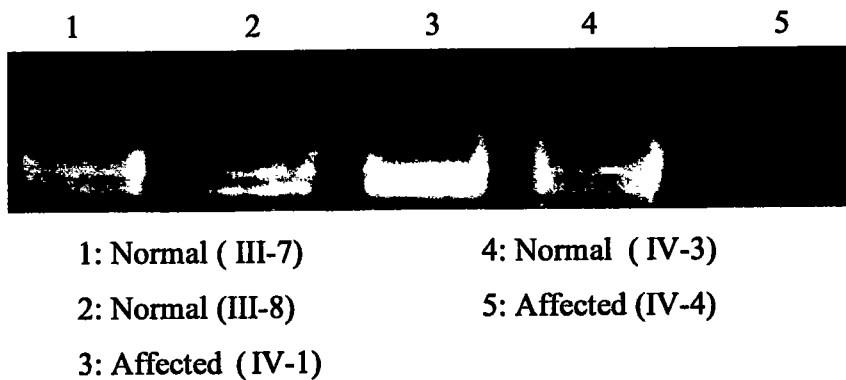
- |                    |                    |
|--------------------|--------------------|
| 1: Normal ( III-7) | 4: Normal ( IV-3)  |
| 2: Normal (III-8)  | 5: Affected (IV-4) |
| 3: Affected (IV-1) |                    |

**Figure 3.11:** Electropherogram of ethidium bromide stained 8% non-denaturing polyacrylamide gel for marker D4S2925 at 7.17 cM chromosome 4p16.3. The Roman numerals indicate the generation number of the individuals within pedigree while Arabic numerals indicate their positions within a generation.

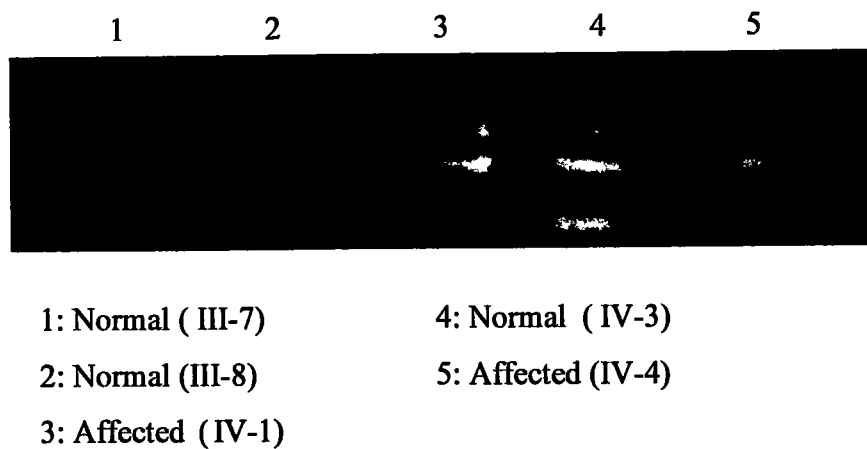
**Family A**

- |                    |                    |
|--------------------|--------------------|
| 1: Normal ( III-7) | 4: Normal ( IV-3)  |
| 2: Normal (III-8)  | 5: Affected (IV-4) |
| 3: Affected (IV-1) |                    |

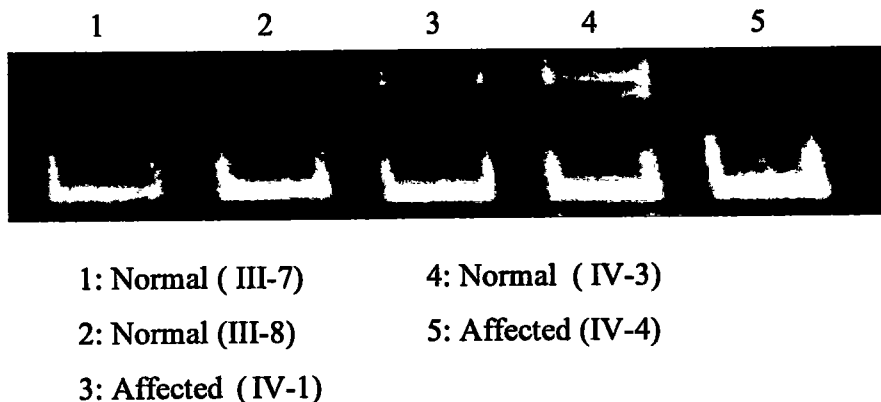
**Figure 3.12:** Electropherogram of ethidium bromide stained 8% non-denaturing polyacrylamide gel for marker D4S394 at 14.94 cM chromosome 4p16.3. The Roman numerals indicate the generation number of the individuals within pedigree while Arabic numerals indicate their positions within a generation.

**Family A: NPR2 (9p21-p12)**

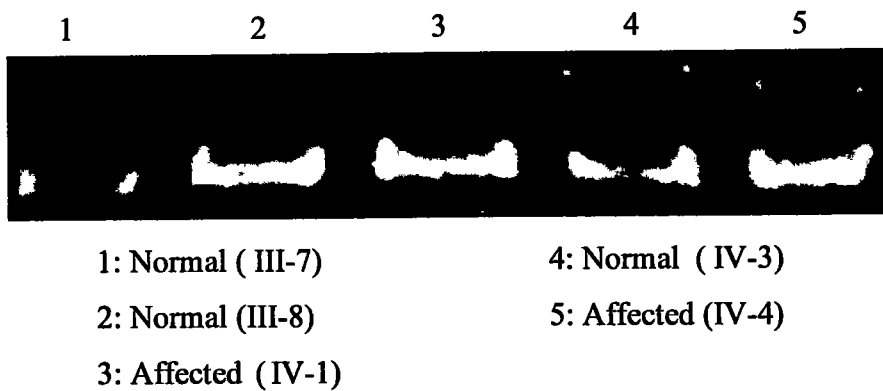
**Figure 3.13:** Electropherogram of ethidium bromide stained 8% non-denaturing polyacrylamide gel for marker D9S1678 at 54.78 cM chromosome 9. The Roman numerals indicate the generation number of the individuals within pedigree while Arabic numerals indicate their positions within a generation.

**Family A**

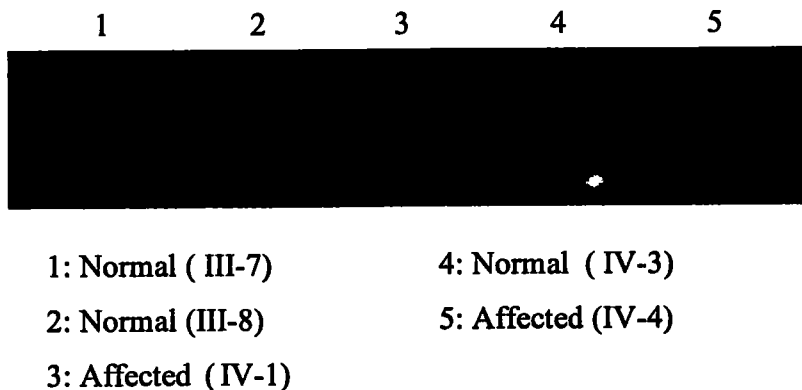
**Figure 3.14:** Electropherogram of ethidium bromide stained 8% non-denaturing polyacrylamide gel for marker D9S319 at 55.51 cM chromosome 9. The Roman numerals indicate the generation number of the individuals within pedigree while Arabic numerals indicate their positions within a generation.

**Family A**

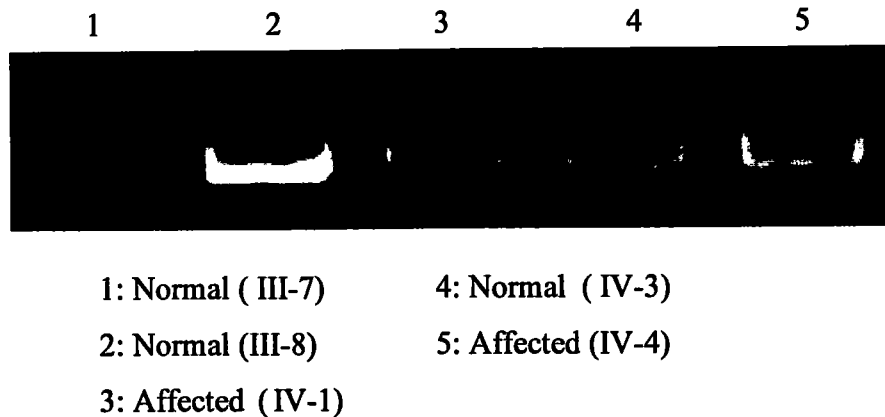
**Figure 3.15:** Electropherogram of ethidium bromide stained 8% non-denaturing polyacrylamide gel for marker D9S1118 at 57.01 cM chromosome 9. The Roman numerals indicate the generation number of the individuals within pedigree while Arabic numerals indicate their positions within a generation.

**Family A**

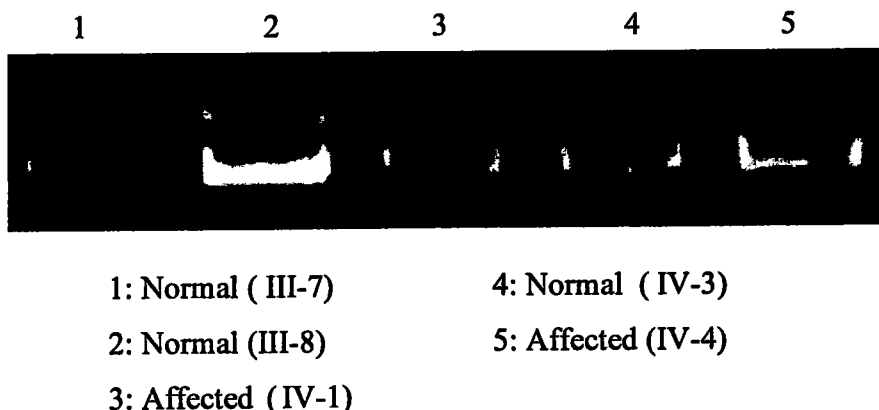
**Figure 3.16:** Electropherogram of ethidium bromide stained 8% non-denaturing polyacrylamide gel for marker D9S1817 at 59cM chromosome 9. The Roman numerals indicate the generation number of the individuals within pedigree while Arabic numerals indicate their positions within a generation.

**Family A**

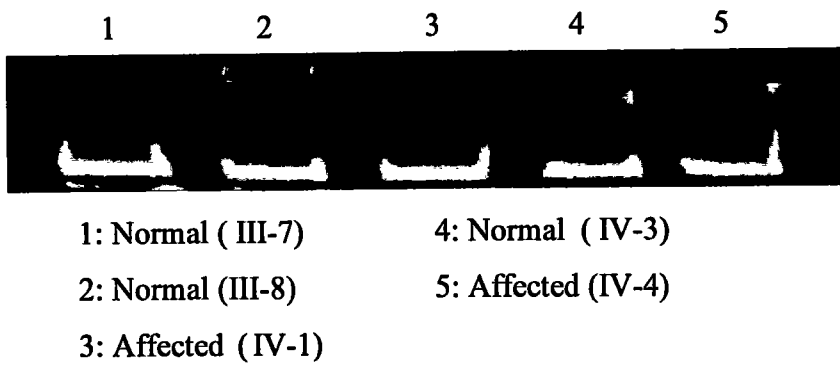
**Figure 3.17:** Electropherogram of ethidium bromide stained 8% non-denaturing polyacrylamide gel for marker D9S1874 at 61.38 cM chromosome 9. The Roman numerals indicate the generation number of the individuals within pedigree while Arabic numerals indicate their positions within a generation.

**Family A**

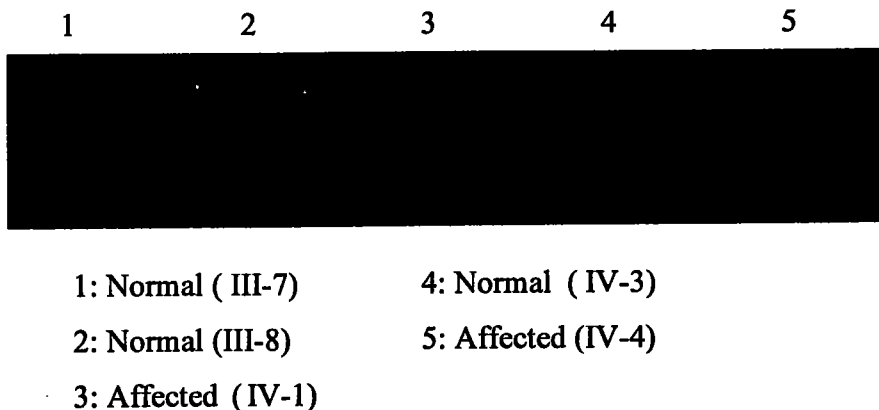
**Figure 3.18:** Electropherogram of ethidium bromide stained 8% non-denaturing polyacrylamide gel for marker D9S55 at 62cM chromosome 9. The Roman numerals indicate the generation number of the individuals within pedigree while Arabic numerals indicate their positions within a generation.

**Family A**

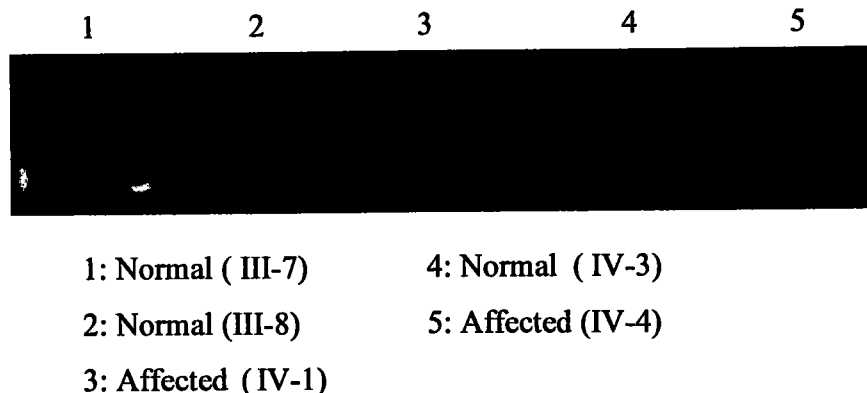
**Figure 3.19:** Electropherogram of ethidium bromide stained 8% non-denaturing polyacrylamide gel for marker D9S773 at 64.28cM chromosome 9. The Roman numerals indicate the generation number of the individuals within pedigree while Arabic numerals indicate their positions within a generation.

**Family A**

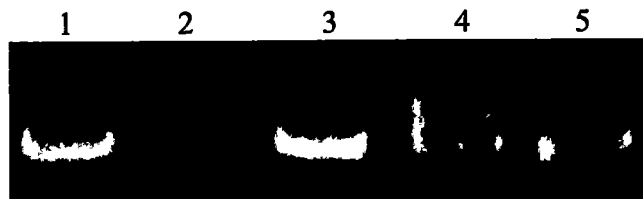
**Figure 3.20:** Electropherogram of ethidium bromide stained 8% non-denaturing polyacrylamide gel for marker D9S1110 at 69cM chromosome 9. The Roman numerals indicate the generation number of the individuals within pedigree while Arabic numerals indicate their positions within a generation.

**Family A: MaP 2K1 (9c)**

**Figure 3.21:** Electropherogram of ethidium bromide stained 8% non-denaturing polyacrylamide gel for marker D9S50 at 60.81 cM chromosome 9. The Roman numerals indicate the generation number of the individuals within pedigree while Arabic numerals indicate their positions within a generation.

**Family A**

**Figure 3.22:** Electropherogram of ethidium bromide stained 8% non-denaturing polyacrylamide gel for marker D9S229 at 62.66 cM chromosome 9. The Roman numerals indicate the generation number of the individuals within pedigree while Arabic numerals indicate their positions within a generation.

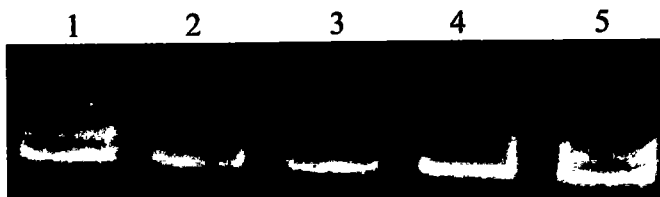
**Family A**

1: Normal ( III-7) 4: Normal ( IV-3)

2: Normal (III-8) 5: Affected (IV-4)

3: Affected ( IV-1)

**Figure 3.23:** Electropherogram of ethidium bromide stained 8% non-denaturing polyacrylamide gel for marker D9S1879 at 66.89 cM chromosome 9q22.32. The Roman numerals indicate the generation number of the individuals within pedigree while Arabic numerals indicate their positions within a generation.

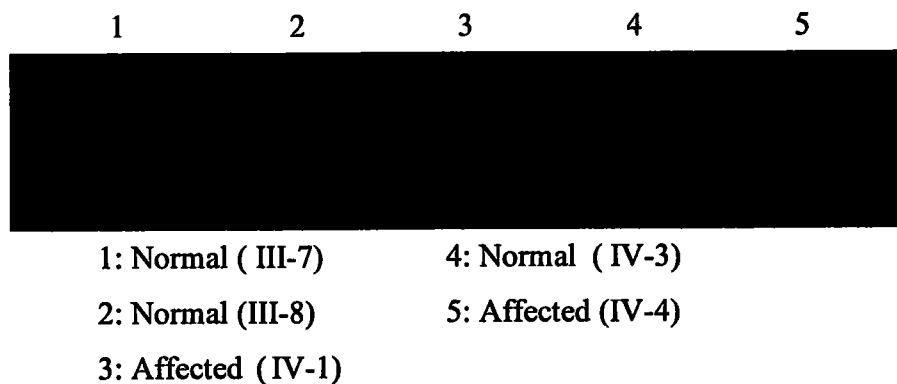
**Family A**

1: Normal ( III-7) 4: Normal ( IV-3)

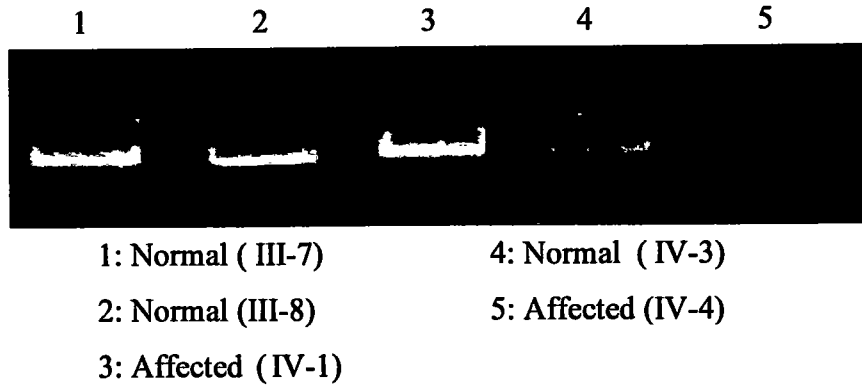
2: Normal (III-8) 5: Affected (IV-4)

3: Affected ( IV-1)

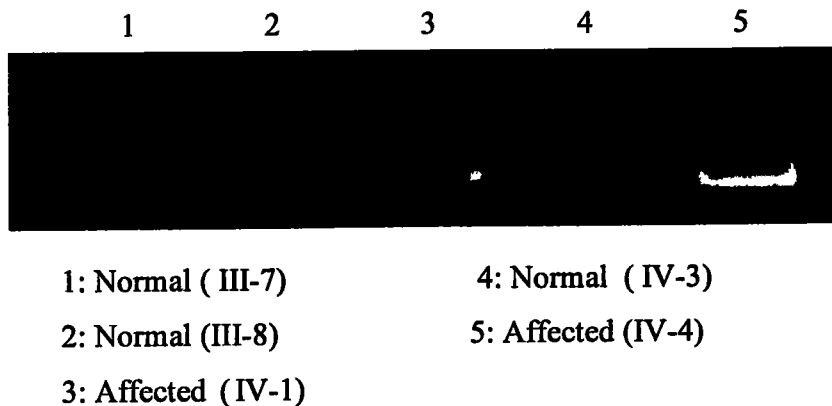
**Figure 3.24:** Electropherogram of ethidium bromide stained 8% non-denaturing polyacrylamide gel for marker D9S15 at 67.37 cM chromosome 9. The Roman numerals indicate the generation number of the individuals within pedigree while Arabic numerals indicate their positions within a generation.

**Family A**

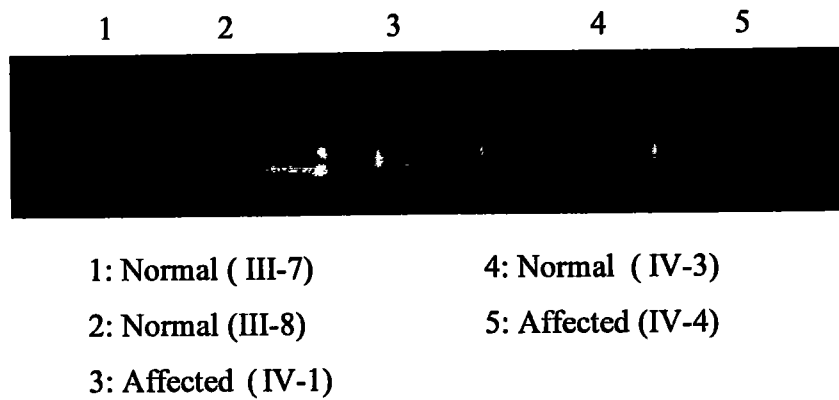
**Figure 3.25:** Electropherogram of ethidium bromide stained 8% non-denaturing polyacrylamide gel for marker D9S1806 at 68.39 cM chromosome 9. The Roman numerals indicate the generation number of the individuals within pedigree while Arabic numerals indicate their positions within a generation.

**Family A**

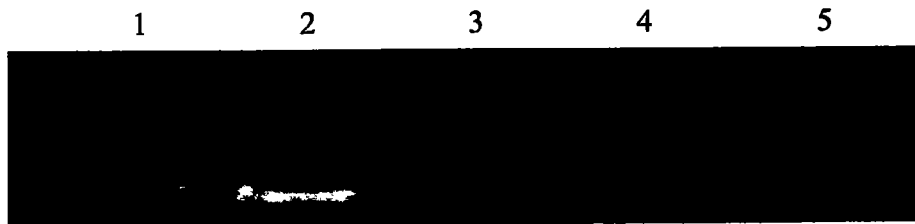
**Figure 3.26:** Electropherogram of ethidium bromide stained 8% non-denaturing polyacrylamide gel for marker D9S1876 at 69.4 cM chromosome 9. The Roman numerals indicate the generation number of the individuals within pedigree while Arabic numerals indicate their positions within a generation.

**Family A: NPPC (2q37.1)**

**Figure 3.27:** Electropherogram of ethidium bromide stained 8% non-denaturing polyacrylamide gel for marker D2S2213 at 236.47 cM chromosome 2. The Roman numerals indicate the generation number of the individuals within pedigree while Arabic numerals indicate their positions within a generation.

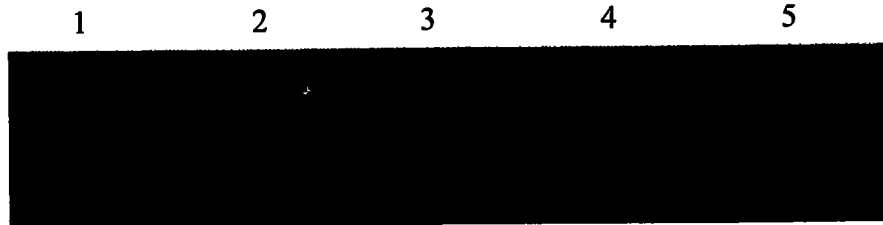
**Family A**

**Figure 3.28:** Electropherogram of ethidium bromide stained 8% non-denaturing polyacrylamide gel for marker D2S396 at 237.40 cM chromosome 2. The Roman numerals indicate the generation number of the individuals within pedigree while Arabic numerals indicate their positions within a generation.

**Family A**

- 1: Normal ( III-7)                          4: Normal ( IV-3)  
2: Normal (III-8)                            5: Affected (IV-4)  
3: Affected ( IV-1)

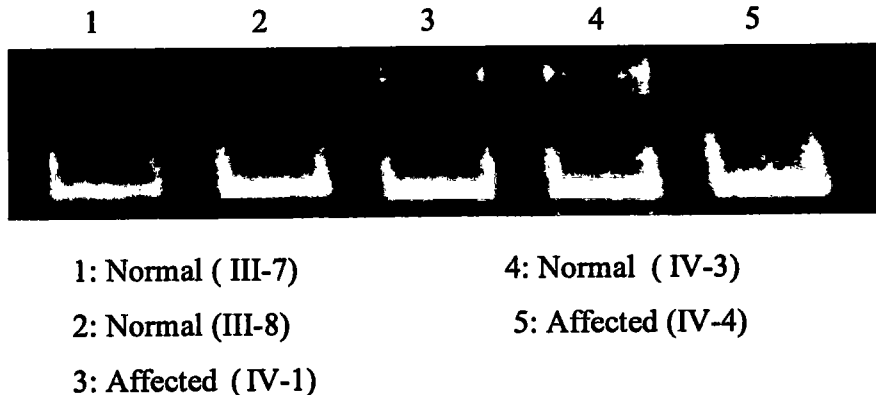
**Figure 3.29:** Electropherogram of ethidium bromide stained 8% non-denaturing polyacrylamide gel for marker D2S2317 at 237.74 cM chromosome 2. The Roman numerals indicate the generation number of the individuals within pedigree while Arabic numerals indicate their positions within a generation.

**Family A**

- 1: Normal ( III-7)                          4: Normal ( IV-3)  
2: Normal (III-8)                            5: Affected (IV-4)  
3: Affected ( IV-1)

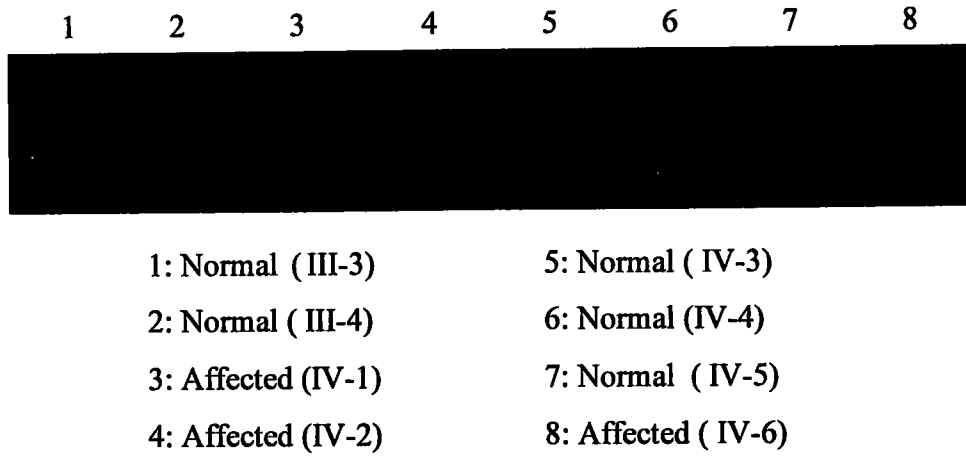
**Figure 3.30:** Electropherogram of ethidium bromide stained 8% non-denaturing polyacrylamide gel for marker D2S427 at 240.12 cM chromosome 2. The Roman numerals indicate the generation number of the individuals within pedigree while Arabic numerals indicate their positions within a generation.

### Family A

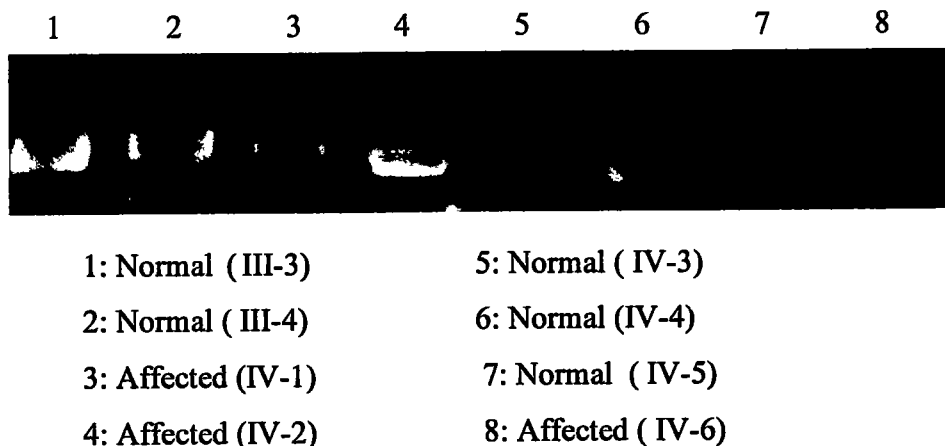


**Figure 3.31:** Electropherogram of ethidium bromide stained 8% non-denaturing polyacrylamide gel for marker D2S2344 at 241.10 cM chromosome 2. The Roman numerals indicate the generation number of the individuals within pedigree while Arabic numerals indicate their positions within a generation.

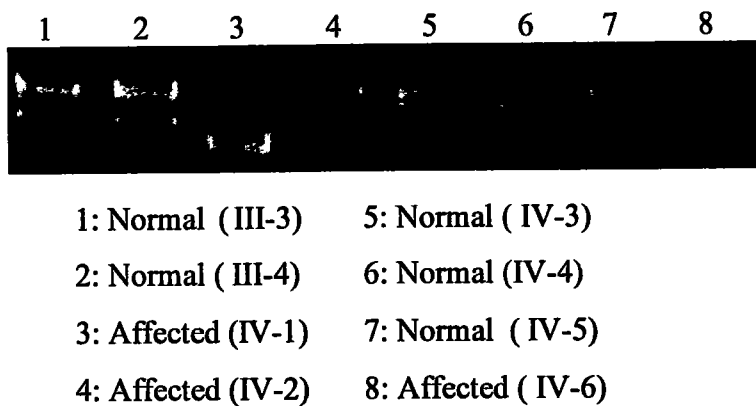
## Family B;IS1



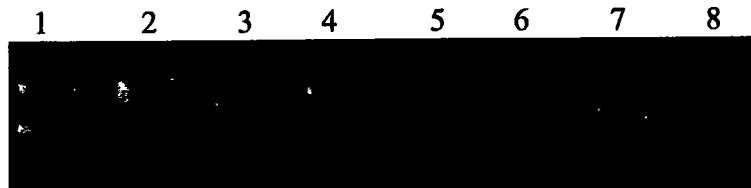
**Figure 3.32:** Electropherogram of ethidium bromide stained 8% non-denaturing polyacrylamide gel for marker D19S894 at 13.95 cM chromosome 19p13.3. The Roman numerals indicate the generation number of the individuals within pedigree while Arabic numerals indicate their positions within a generation.

**Family B**

**Figure 3.33:** Electropherogram of ethidium bromide stained 8% non-denaturing polyacrylamide gel for marker D19S1034 at 18.216 cM chromosome 19p13.3. The Roman numerals indicate the generation number of the individuals within pedigree while Arabic numerals indicate their positions within a generation.

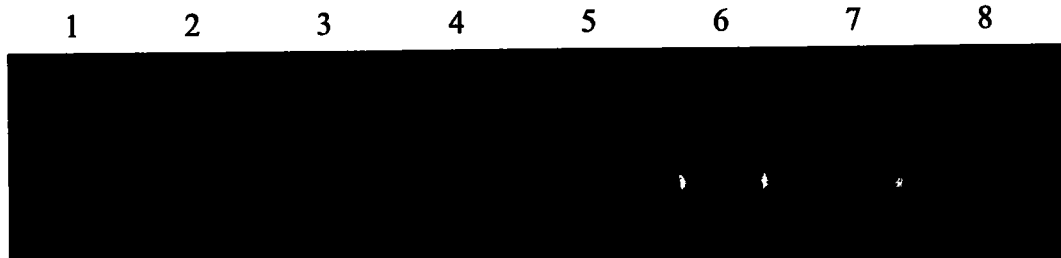
**Family B**

**Figure 3.34:** Electropherogram of ethidium bromide stained 8% non-denaturing polyacrylamide gel for marker D19S567 at 22.98 cM chromosome 19p13.3. The Roman numerals indicate the generation number of the individuals within pedigree while Arabic numerals indicate their positions within a generation.

**Family B**

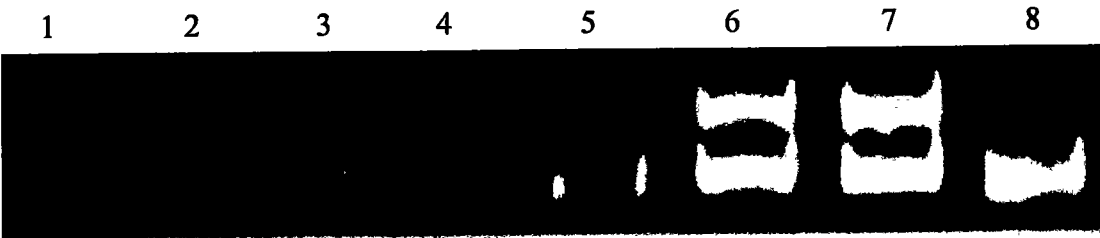
- |                    |                    |
|--------------------|--------------------|
| 1: Normal (III-3)  | 5: Normal (IV-3)   |
| 2: Normal (III-4)  | 6: Normal (IV-4)   |
| 3: Affected (IV-1) | 7: Normal (IV-5)   |
| 4: Affected (IV-2) | 8: Affected (IV-6) |

**Figure 3.35:** Electropherogram of ethidium bromide stained 8% non-denaturing polyacrylamide gel for marker D19S884 at 23.6 cM chromosome 19p13.3. The Roman numerals indicate the generation number of the individuals within pedigree while Arabic numerals indicate their positions within a generation.

**Family B**

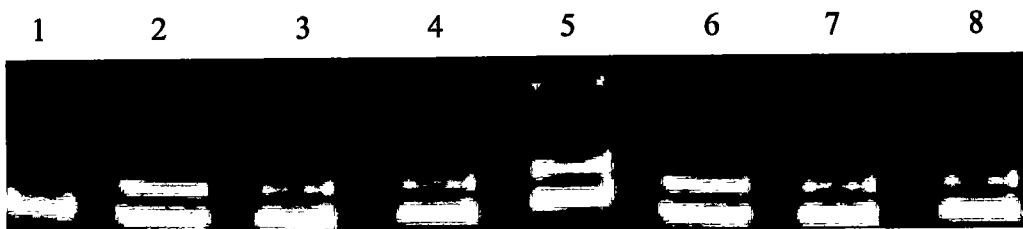
- |                    |                    |
|--------------------|--------------------|
| 1: Normal (III-3)  | 5: Normal (IV-3)   |
| 2: Normal (III-4)  | 6: Normal (IV-4)   |
| 3: Affected (IV-1) | 7: Normal (IV-5)   |
| 4: Affected (IV-2) | 8: Affected (IV-6) |

**Figure 3.36:** Electropherogram of ethidium bromide stained 8% non-denaturing polyacrylamide gel for marker D19S916 at 27.33 cM chromosome 19p13.3. The Roman numerals indicate the generation number of the individuals within pedigree while Arabic numerals indicate their positions within a generation.

**Family B**

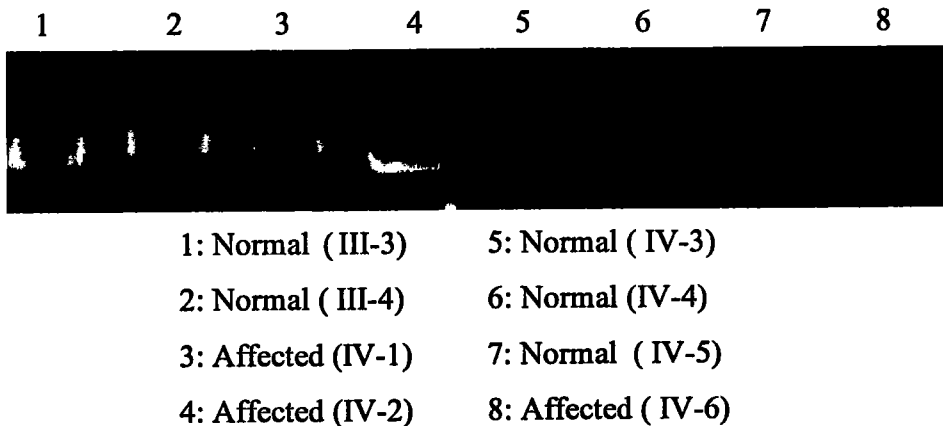
- |                    |                     |
|--------------------|---------------------|
| 1: Normal ( III-3) | 5: Normal ( IV-3)   |
| 2: Normal ( III-4) | 6: Normal (IV-4)    |
| 3: Affected (IV-1) | 7: Normal ( IV-5)   |
| 4: Affected (IV-2) | 8: Affected ( IV-6) |

**Figure 3.37:** Electropherogram of ethidium bromide stained 8% non-denaturing polyacrylamide gel for marker D19S865 at 28.23cM chromosome 19p13.3. The Roman numerals indicate the generation number of the individuals within pedigree while Arabic numerals indicate their positions within a generation.

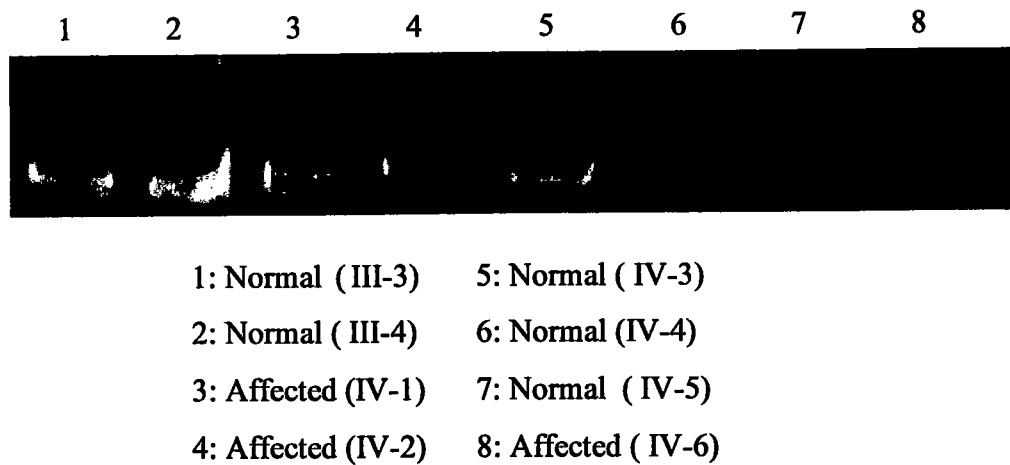
**Family B**

- |                    |                     |
|--------------------|---------------------|
| 1: Normal ( III-3) | 5: Normal ( IV-3)   |
| 2: Normal ( III-4) | 6: Normal (IV-4)    |
| 3: Affected (IV-1) | 7: Normal ( IV-5)   |
| 4: Affected (IV-2) | 8: Affected ( IV-6) |

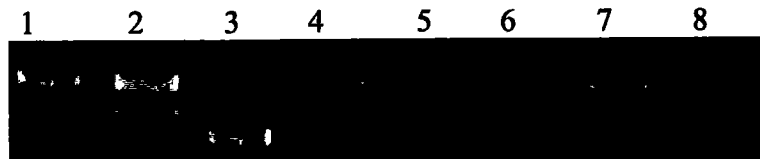
**Figure 3.38:** Electropherogram of ethidium bromide stained 8% non-denaturing polyacrylamide gel for marker D19S221 at 32.91 cM chromosome 19p13.3. The Roman numerals indicate the generation number of the individuals within pedigree while Arabic numerals indicate their positions within a generation.

**Family B;IS2**

**Figure 3.39:** Electropherogram of ethidium bromide stained 8% non-denaturing polyacrylamide gel for marker D17S1856 at 39.76 cM chromosome 17p11. The Roman numerals indicate the generation number of the individuals within pedigree while Arabic numerals indicate their positions within a generation.

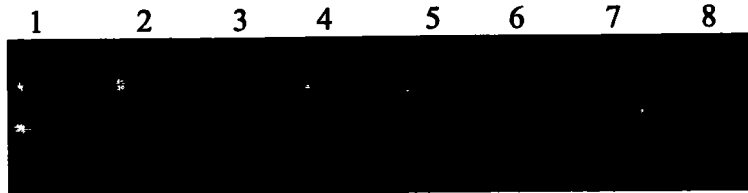
**Family B**

**Figure 3.40:** Electropherogram of ethidium bromide stained 8% non-denaturing polyacrylamide gel for marker D17S839 at 41.92 cM chromosome 17p11. The Roman numerals indicate the generation number of the individuals within pedigree while Arabic numerals indicate their positions within a generation

**Family B**

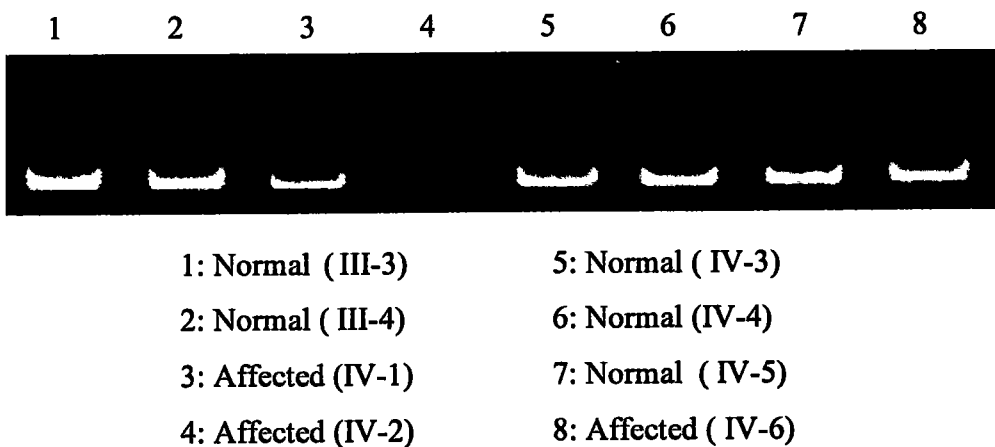
1: Normal (III-3)	5: Normal (IV-3)
2: Normal (III-4)	6: Normal (IV-4)
3: Affected (IV-1)	7: Normal (IV-5)
4: Affected (IV-2)	8: Affected (IV-6)

**Figure 3.41:** Electropherogram of ethidium bromide stained 8% non-denaturing polyacrylamide gel for marker D17S1843 at 45.95 cM chromosome 17p11. The Roman numerals indicate the generation number of the individuals within pedigree while Arabic numerals indicate their positions within a generation.

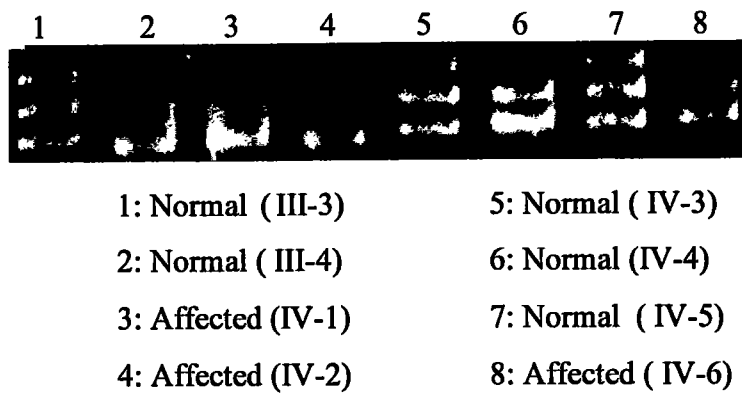
**Family B**

1: Normal (III-3)	5: Normal (IV-3)
2: Normal (III-4)	6: Normal (IV-4)
3: Affected (IV-1)	7: Normal (IV-5)
4: Affected (IV-2)	8: Affected (IV-6)

**Figure 3.42:** Electropherogram of ethidium bromide stained 8% non-denaturing polyacrylamide gel for marker D17S2196 at 47.28cM chromosome 17p11. The Roman numerals indicate the generation number of the individuals within pedigree while Arabic numerals indicate their positions within a generation

**Family B**

**Figure 3.43:** Electropherogram of ethidium bromide stained 8% non-denaturing polyacrylamide gel for marker D17S842 at 49.4 cM chromosome 17p11. The Roman numerals indicate the generation number of the individuals within pedigree while Arabic numerals indicate their positions within a generation.

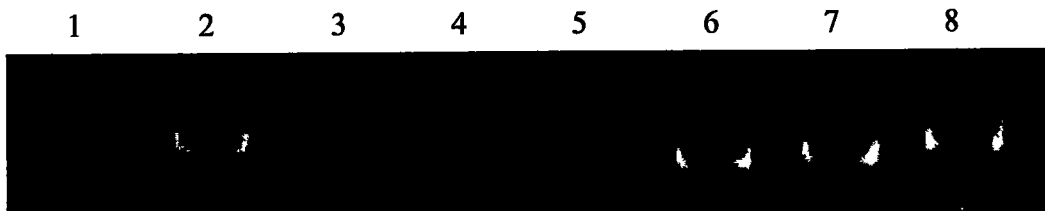
**Family B**

**Figure 3.44:** Electropherogram of ethidium bromide stained 8% non-denaturing polyacrylamide gel for marker D17S783 at 50.54 chromosome 17p11. The Roman numerals indicate the generation number of the individuals within pedigree while Arabic numerals indicate their positions within a generation.

**Family B**

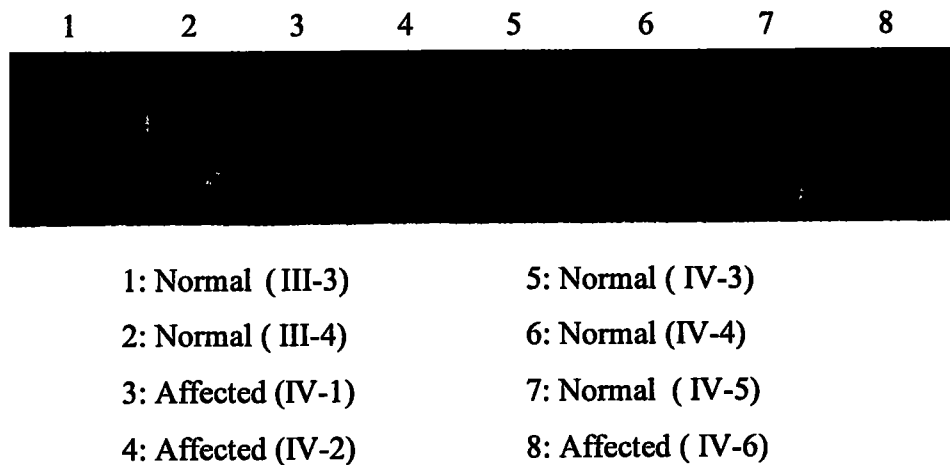
- |                    |                    |
|--------------------|--------------------|
| 1: Normal (III-3)  | 5: Normal (IV-3)   |
| 2: Normal (III-4)  | 6: Normal (IV-4)   |
| 3: Affected (IV-1) | 7: Normal (IV-5)   |
| 4: Affected (IV-2) | 8: Affected (IV-6) |

**Figure 3.45:** Electropherogram of ethidium bromide stained 8% non-denaturing polyacrylamide gel for marker D17S1878 at 51.2 cM chromosome 17p11. The Roman numerals indicate the generation number of the individuals within pedigree while Arabic numerals indicate their positions within a generation.

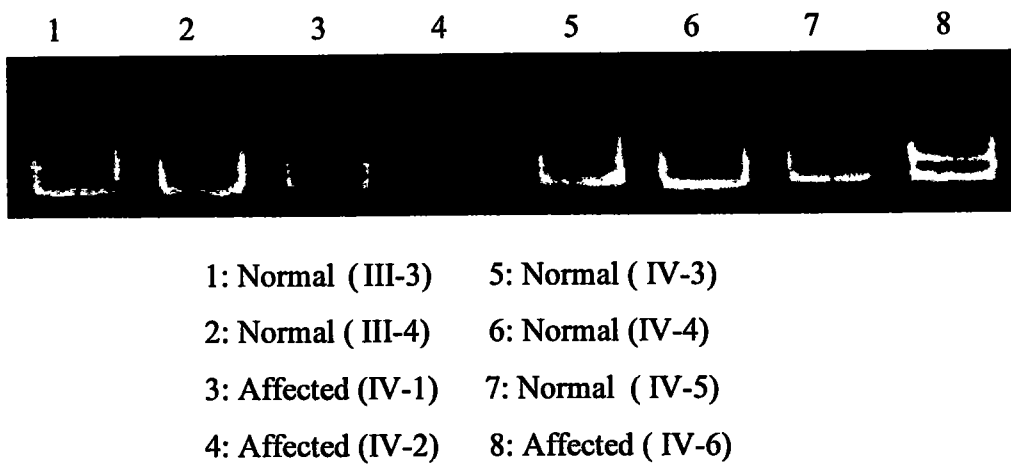
**Family B**

- |                    |                    |
|--------------------|--------------------|
| 1: Normal (III-3)  | 5: Normal (IV-3)   |
| 2: Normal (III-4)  | 6: Normal (IV-4)   |
| 3: Affected (IV-1) | 7: Normal (IV-5)   |
| 4: Affected (IV-2) | 8: Affected (IV-6) |

**Figure 3.46:** Electropherogram of ethidium bromide stained 8% non-denaturing polyacrylamide gel for marker D17S1800 at 53.14cM chromosome 17p11. The Roman numerals indicate the generation number of the individuals within pedigree while Arabic numerals indicate their positions within a generation.

**Family B;IS3**

**Figure 3.47:** Electropherogram of ethidium bromide stained 8% non-denaturing polyacrylamide gel for marker D8S1471 at 122.32 cM chromosome 8q12. The Roman numerals indicate the generation number of the individuals within pedigree while Arabic numerals indicate their positions within a generation.

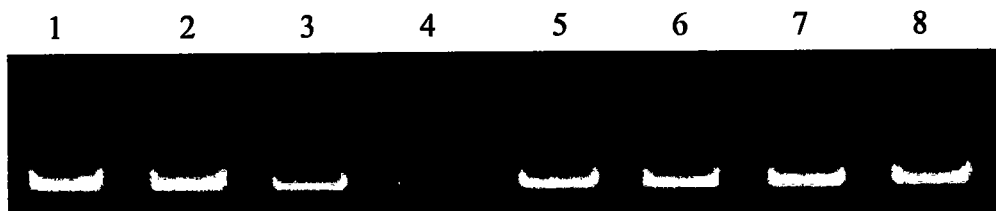
**Family B**

**Figure 3.48:** Electropherogram of ethidium bromide stained 8% non-denaturing polyacrylamide gel for marker D8S565 at 123.01 cM chromosome 8q12. The Roman numerals indicate the generation number of the individuals within pedigree while Arabic numerals indicate their positions within a generation.

**Family B**

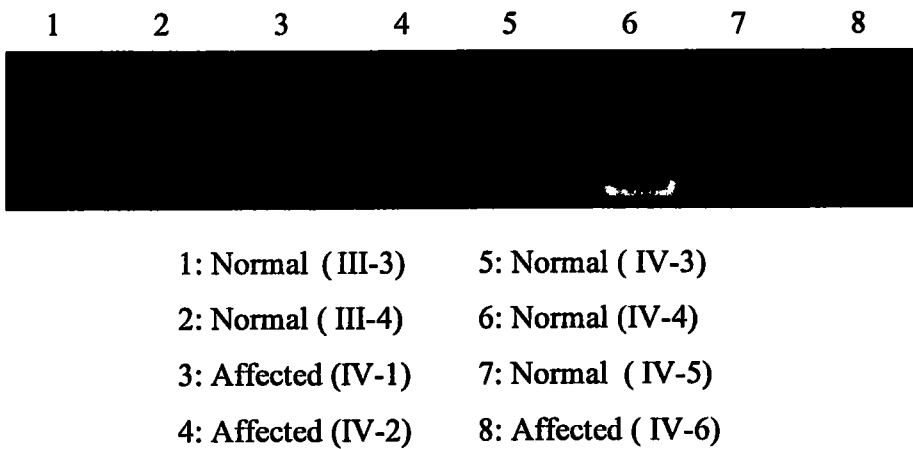
- |                    |                    |
|--------------------|--------------------|
| 1: Normal (III-3)  | 5: Normal (IV-3)   |
| 2: Normal (III-4)  | 6: Normal (IV-4)   |
| 3: Affected (IV-1) | 7: Normal (IV-5)   |
| 4: Affected (IV-2) | 8: Affected (IV-6) |

**Figure 3.49:** Electropherogram of ethidium bromide stained 8% non-denaturing polyacrylamide gel for marker D8S592 at 124.85 cM chromosome 8q12. The Roman numerals indicate the generation number of the individuals within pedigree while Arabic numerals indicate their positions within a generation.

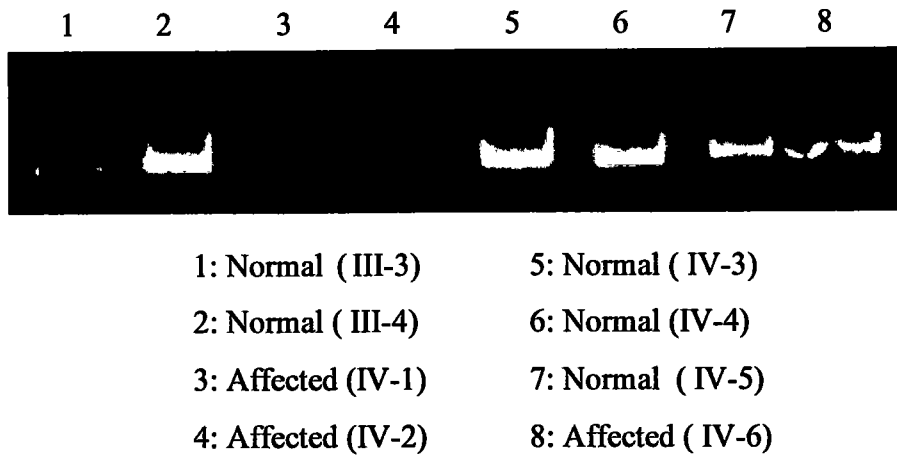
**Family B**

- |                    |                    |
|--------------------|--------------------|
| 1: Normal (III-3)  | 5: Normal (IV-3)   |
| 2: Normal (III-4)  | 6: Normal (IV-4)   |
| 3: Affected (IV-1) | 7: Normal (IV-5)   |
| 4: Affected (IV-2) | 8: Affected (IV-6) |

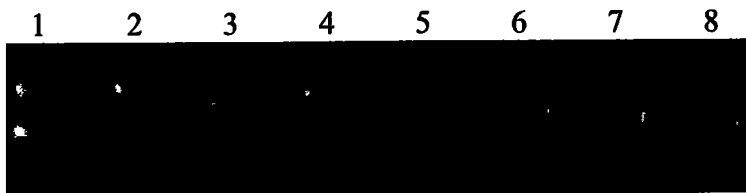
**Figure 3.50:** Electropherogram of ethidium bromide stained 8% non-denaturing polyacrylamide gel for marker D8S527 at 214.40 cM chromosome 2q34-q36. The Roman numerals indicate the generation number of the individuals within pedigree while Arabic numerals indicate their positions within a generation.

**Family B**

**Figure 3.51:** Electropherogram of ethidium bromide stained 8% non-denaturing polyacrylamide gel for marker D8S199 at 27.33 cM chromosome 19p13.3. The Roman numerals indicate the generation number of the individuals within pedigree while Arabic numerals indicate their positions within a generation.

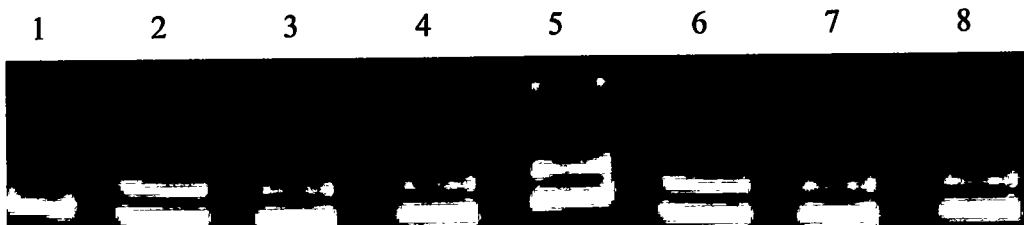
**Family B IS4**

**Figure 3.52:** Electropherogram of ethidium bromide stained 8% non-denaturing polyacrylamide gel for marker D9S1105 at 119 cM chromosome 19p13.3. The Roman numerals indicate the generation number of the individuals within pedigree while Arabic numerals indicate their positions within a generation.

**Family B**

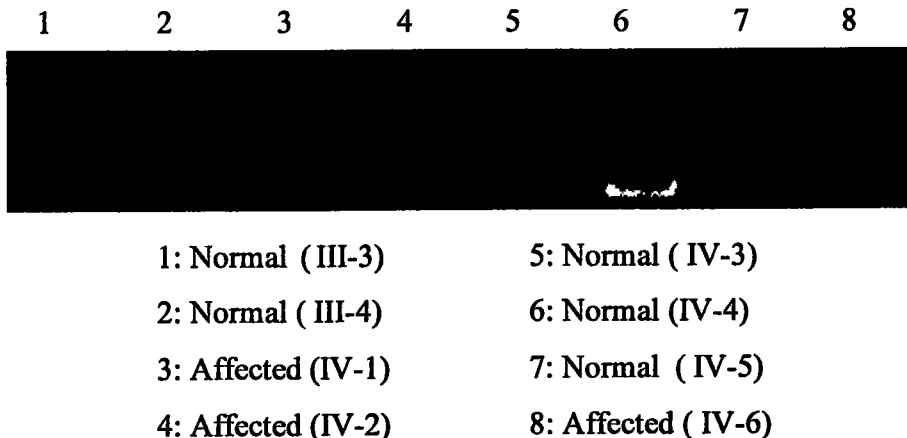
- |                    |                    |
|--------------------|--------------------|
| 1: Normal (III-3)  | 5: Normal (IV-3)   |
| 2: Normal (III-4)  | 6: Normal (IV-4)   |
| 3: Affected (IV-1) | 7: Normal (IV-5)   |
| 4: Affected (IV-2) | 8: Affected (IV-6) |

**Figure 3.53:** Electropherogram of ethidium bromide stained 8% non-denaturing polyacrylamide gel for marker D9S1776 at 123.79 cM chromosome 9q31.2-34.2. The Roman numerals indicate the generation number of the individuals within pedigree while Arabic numerals indicate their positions within a generation.

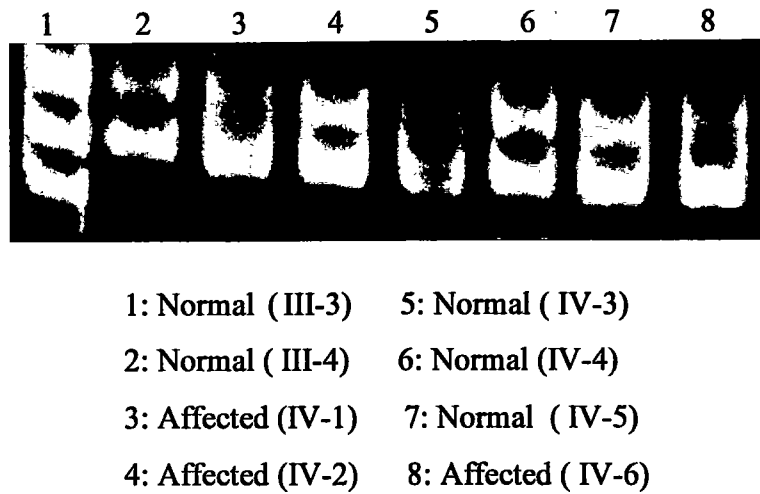
**Family B**

- |                    |                    |
|--------------------|--------------------|
| 1: Normal (III-3)  | 5: Normal (IV-3)   |
| 2: Normal (III-4)  | 6: Normal (IV-4)   |
| 3: Affected (IV-1) | 7: Normal (IV-5)   |
| 4: Affected (IV-2) | 8: Affected (IV-6) |

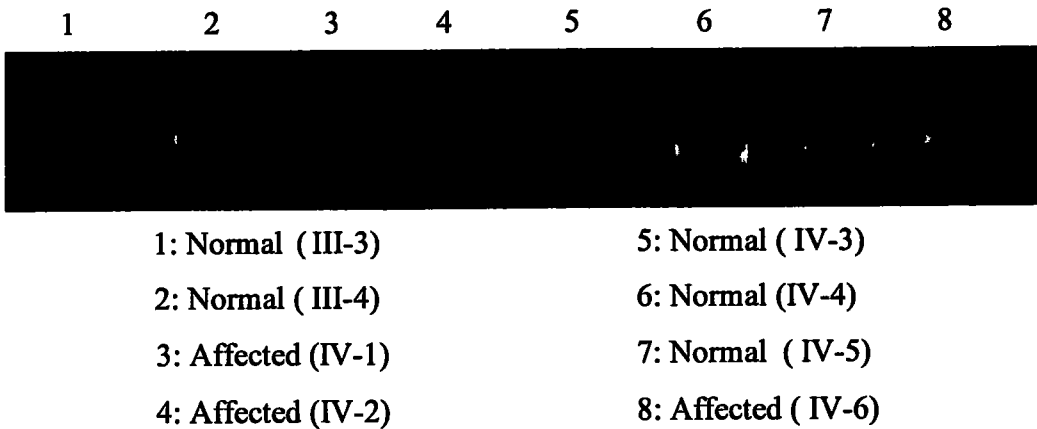
**Figure 3.54:** Electropherogram of ethidium bromide stained 8% non-denaturing polyacrylamide gel for marker D9S1685 at 132.42 cM chromosome 9q31.2-34.2. The Roman numerals indicate the generation number of the individuals within pedigree while Arabic numerals indicate their positions within a generation.

**Family B**

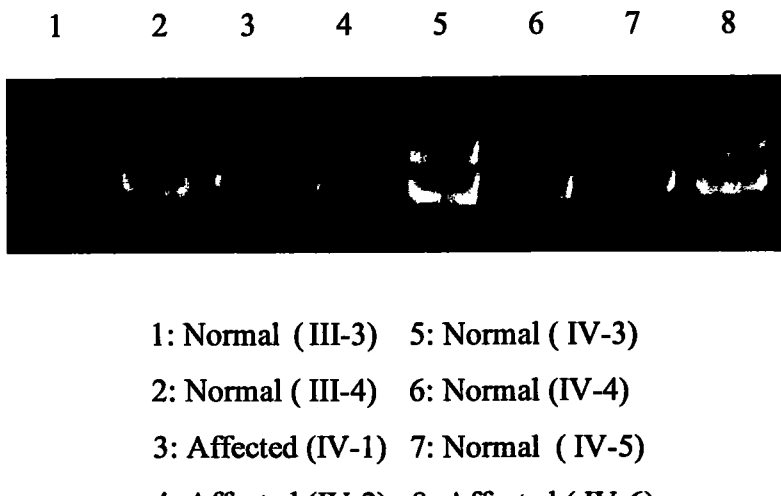
**Figure 3.55:** Electropherogram of ethidium bromide stained 8% non-denaturing polyacrylamide gel for marker D9S290 at 139.74cM chromosome9q31.2-34.2. The Roman numerals indicate the generation number of the individuals within pedigree while Arabic numerals indicate their positions within a generation

**Family B**

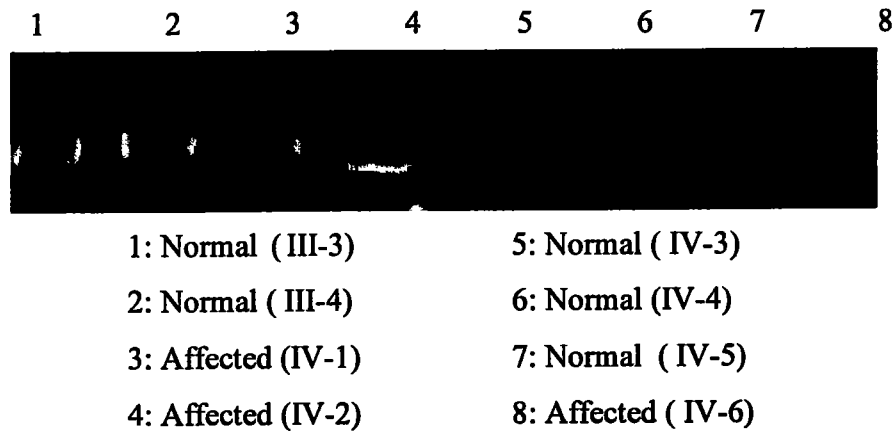
**Figure 3.56:** Electropherogram of ethidium bromide stained 8% non-denaturing polyacrylamide gel for marker D9S766 at 142 cM chromosome9q31.2-34.2. The Roman numerals indicate the generation number of the individuals within pedigree while Arabic numerals indicate their positions within a generation.

**Family B**

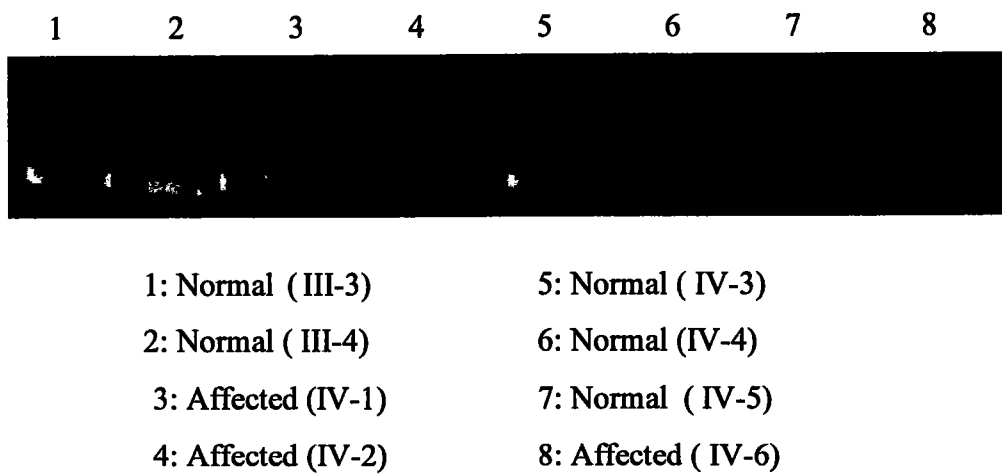
**Figure 3.57:** Electropherogram of ethidium bromide stained 8% non-denaturing polyacrylamide gel for marker D9S1793 at 149.91 cM chromosome 9q31.2-34.2. The Roman numerals indicate the generation number of the individuals within pedigree while Arabic numerals indicate their positions within a generation.

**Family B;IS5**

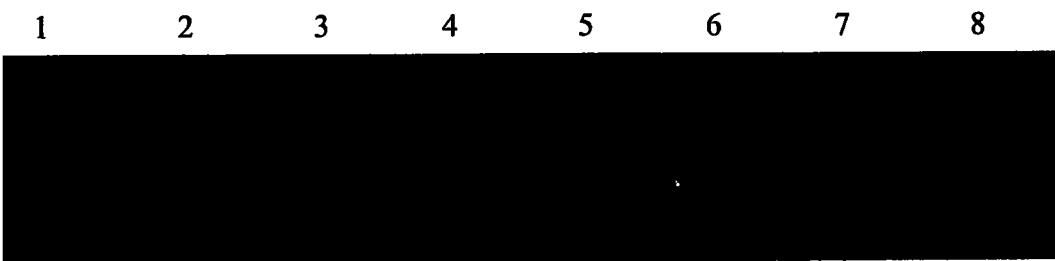
**Figure 3.58:** Electropherogram of ethidium bromide stained 8% non-denaturing polyacrylamide gel for marker D17S1847 at 122 cM chromosome 17q25.3-qter. The Roman numerals indicate the generation number of the individuals within pedigree while Arabic numerals indicate their positions within a generation.

**Family B**

**Figure 3.59:** Electropherogram of ethidium bromide stained 8% non-denaturing polyacrylamide gel for marker D17S1806 at 125 cM chromosome 17q25.3-qter. The Roman numerals indicate the generation number of the individuals within pedigree while Arabic numerals indicate their positions within a generation.

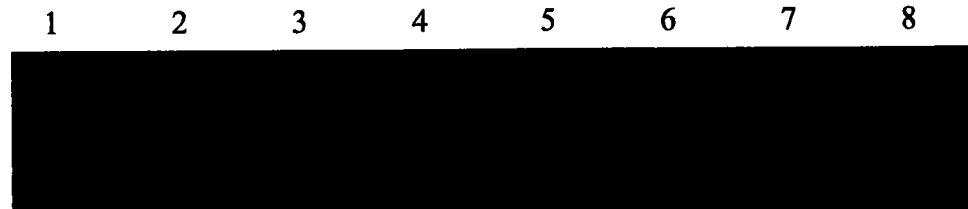
**Family B**

**Figure 3.60:** Electropherogram of ethidium bromide stained 8% non-denaturing polyacrylamide gel for marker D17S784 at 127.8 cM chromosome 17q25.3-qter. The Roman numerals indicate the generation number of the individuals within pedigree while Arabic numerals indicate their positions within a generation.

**Family B**

- |                    |                    |
|--------------------|--------------------|
| 1: Normal (III-3)  | 5: Normal (IV-3)   |
| 2: Normal (III-4)  | 6: Normal (IV-4)   |
| 3: Affected (IV-1) | 7: Normal (IV-5)   |
| 4: Affected (IV-2) | 8: Affected (IV-6) |

**Figure 3.61:** Electropherogram of ethidium bromide stained 8% non-denaturing polyacrylamide gel for marker D17S914 at 131.07 cM chromosome 17q25.3-qter. The Roman numerals indicate the generation number of the individuals within pedigree while Arabic numerals indicate their positions within a generation.

**Family B**

- |                    |                    |
|--------------------|--------------------|
| 1: Normal (III-3)  | 5: Normal (IV-3)   |
| 2: Normal (III-4)  | 6: Normal (IV-4)   |
| 3: Affected (IV-1) | 7: Normal (IV-5)   |
| 4: Affected (IV-2) | 8: Affected (IV-6) |

**Figure 3.62:** Electropherogram of ethidium bromide stained 8% non-denaturing polyacrylamide gel for marker D17S668 at 133.61 cM chromosome 17q25.3-qter. The Roman numerals indicate the generation number of the individuals within pedigree while Arabic numerals indicate their positions within a generation

# **CHAPTER 4**

# **DISCUSSION**

## Discussion

Skeletal dysplasia are a group of heterogeneous genetic disorders associated with a generalized abnormality of skeletal growth affecting bones and cartilage. Today, there are more than 456 well characterized skeletal dysplasia classified primarily on the basis of clinical, radiographic, and molecular criteria. Genetic disorders involving the skeletal system arise from disturbances in the complex processes of skeletal development, growth and homeostasis (Warman *et al.*, 2010). A variety of genes are expressed during normal development of skeleton in different stages of growth plate, chondrocyte development, and their protein products play crucial roles in cell differentiation or patterning (McInnes and Michaud., 2008). Skeletal dysplasia are caused by genetic mutations and can run in families. Often the disorders appear without any family history of skeletal dysplasia. According to Warman *et al* (2010), 316 out of 456 different conditions of skeletal dysplasia were associated with mutations in one or more of 226 different genes. Involvement of many genes in skeletal development makes it difficult to delineate the role of an individual gene in a particular genetic skeletal dysplasia. (Deborah *et al.*,2009) In the present study, two families (A and B) with different types of skeletal dysplasia were included and subjected to linkage analysis. Affected individuals in family A showed characteristic features of achondroplasia ,disproportionately short limbs, macrocephaly, three pronged fingers (trident) and characteristic facial features with depressed nasal bridge, frontal bossing and mid-face hypoplasia (Trotter and Hall, 2005). No other associated abnormality was found in affected individuals. Adolescent idiopathic scoliosis (AIS) was phenotype of family B , characterize by complex spinal abnormality along with axial rotation ,of unknown cause and lateral curvature  $>10^\circ$ (Czeizel *et al* .,1978).No other associated abnormality was found in affected individuals and consanguineous marriages were observed in family B.

To track the gene responsible for monogenetic recessive skeletal dysplasia, homozygosity mapping technique was used. Homozygosity mapping is based on the principle that a particular portion of genome of siblings from consanguineous marriages would be homozygous because of identity by descent (IBD). One-sixteenth part of genome of offspring from first cousin marriages is expected to be homozygous (Sheffield *et al.*, 1995).

That particular region of homozygosity is random between different offsprings of these cousin marriages except for a definite disease locus that is exclusively shared and common between all affected siblings.

Linkage analysis was carried out on two families (A and B) by typing highly polymorphic microsatellite markers to candidate genes, involved in respective hereditary skeletal dysplasia. If a family showed a convincing linkage to a candidate gene then sequencing analysis would be performed to identify any pathogenic sequence variant. Genotyping of family A with autosomal recessive achondroplasias was carried out by typing microsatellite markers to, FGFR3, NPR2, MaP2K1 and NPPC genes. FGFR3 is most important gene involved in achondroplasias. FGFR3 is actually negative regulator of skeletal growth, which restricts the length of the epiphyseal plates of long bones via inhibition of chondrocyte proliferation. Mutation in FGFR3 gene causes achondroplasia and range of skeletal dysplasia disorders (Richette *et al.*, 2008). While NPR2, MaP2K1 and NPPC genes are less common in achondroplasias. Genotyping with highly polymorphic microsatellite markers for investigation of linkage with known genes showed that affected individuals were heterozygous for different combinations of parental alleles, thus excluding linkage to known hereditary candidate genes in family A. This concluded that a novel gene must be responsible for causing achondroplasia in family A. In family B, genotyping with highly polymorphic microsatellite markers for investigation of linkage with known adolescent idiopathic scoliosis loci showed that heterozygosity for different combinations of parental alleles in affected individuals. Thus family B was excluded from known loci involved in idiopathic scoliosis, suggesting the involvement of a novel gene in adolescent idiopathic scoliosis of family B.

Aim of the present study was to identify the genes/ loci involved in inherited skeletal dysplasia and to investigate disease pathogenesis at molecular level. It will help to develop a community-generated knowledge base that will significantly improve diagnosis, treatment, management and understanding of skeletal dysplasia and related disorders. This study will support an international network of patients, clinicians and researchers seeking a better understanding of skeletal dysplasia and provides further insight in molecular pathogenesis and target for treatment.

# **CHAPTE 5**

# **REFERENCES**

## REFERENCES

- Adobor R.D., Joranger P., Steen H., Navrud S., And Brox J.I., (2014) A health economic evaluation of screening and treatment in patients with adolescent idiopathic scoliosis. *Scoliosis*, 9(21), 13013-014-0021-8
- Alanay Y., Avaygan H., Camacho N., Utine GE., Boduroglu K., Aktas D., Tuncbilek E., Orhan D., Bakar F.T., Zabel B., Superti-Furga A., Bruckner- Tuderman L., Curry C.J., Pyott S., Byers P.H., Eyre D.R., Baldridge D., Lee B., Merrill A.E., Davis E.C., Cohn D.H., Akarsu N., And Krakow D., (2010) Mutations in the gene encoding the RER protein FKBP65 cause autosomal-recessive osteogenesis imperfect, *Am J Hum Genet* ,86, 551-559
- Alanay Y., And Lachman S.R., (2011) A Review of the Principles of Radiological Assessment of Skeletal Dysplasia ,*Res Pediatr Endocrinol*,3(4),163-17.
- Barnes A.M., Chang W., Morello R., Cabral W.A., Weis M., Eyre D.R., Leikin S., Makareeva E., Kuznetsova N., Uveges T.E., Ashok A., Flor A.W., Mulvihill J.J., Wilson P.L., Sundaram U.T., Lee B., And Marini J.C., (2006) Deficiency of cartilage associated protein in recessive lethal osteogenesis imperfect, *N Engl J Med*,355, 2757-2764
- Bellus G.A., Gaudenz K., Zackai E.H., Clarke L.A., Szabo J., Francomano C.A., And Muenke M (1996) Identical mutations in three different fibroblast growth factor receptor genes in autosomal dominant craniosynostosis syndromes, *Nat J Genet*, 14, 174-176
- Ben Amor I.M., Glorieux F.H., And Rauch F., (2011) Genotype-phenotype correlations in autosomal dominant osteogenesis imperfect, *J Osteoporos*,35 ,540178
- Bennett R.L., Steinhaus K.A., Uhrich S.B., O'Sullivan C.K., Resta R.G., Lochner-Doyle D., Markel D.S., Vincet V., And Hamanishi J., (1995) Recommendations for standardized human pedigree nomenclature, Pedigree standardization task force of the national society of genetic counselors, *Am J Hum Genet*, 56, 745-752

- Berger A., Haschke N., Kohlhauser C., Amman G., Unterberger U., Weninger M., (1998) Neonatal cholestasis and focal medullary dysplasia of the kidneys in a case of microcephalic osteodysplastic primordial dwarfism, *J Med Genet* 35,61-64
- Bhardwaj G, Murdoch B, Wu D., Baker D.P, Williams K.P, Chadwick K, Ling L.E, Karanu FN, Bhatia M (2001) Sonic hedgehog induces the proliferation of primitive human hematopoietic cells via BMP regulation, *Nat Immun* 2, 172-180
- Bianchi D.W., Crombleholme TM., And D'Alton M.E., (2000) Diastrophic dysplasia. In *Fetology. Diagnosis & Management of the Fetal Patient*, McGraw-Hill NY, 697-703
- Bodian D.L., Chan T.F., Poon A., Schwarze U., Yang K., Byers P.H., Kwok P.Y., Klein T.E.,(2009) Mutation and polymorphism spectrum in osteogenesis imperfecta type II: implications for genotype-phenotype relationships, *Hum Mol Genet*, 18,463-471
- Bosse K., Betz R.C, Lee Y.A., Wienker T.F., Reis A., Kleen H., Propping P., Cichon S, Nothen M.M., (2000) Localization of a gene for syndactyly type 1 to Chromosome 2q34-q36. *Am J Hum Genet* 67, 492-497
- Bradbury J.A., Martin L., Strachan I.M., (1987) Acquired Brown's syndrome associated with Hurler-Scheie's syndrome, *Br J Ophthalmol* 73, 305-308
- Colvin J.S., Bohne B.A., Harding G.W., McEwen D.G., And Ornitz D.M (1996) Skeletal overgrowth and deafness in mice lacking fibroblast growth factor receptor 3. *Nat Genet* 12,390-397
- Coutinho M.F., Lacerda L.U., Alves S., (2011) Glycosaminoglycan Storage Disorders: a review, *Biochem Res Int* 5, 1-16
- Czeizel A., Bellyei A., O Barta O., Magda Tand L., Molnár L., (1978) Genetics of adolescent idiopathic scoliosis, *J Med Genet*, 15,424-427

- Edery P., Jeannin P.M., Biot B., Labalme A., Bernard J. C., Chastang L., Kassai.B., and Plais M.H., (2011). New disease gene location and high genetic heterogeneity in idiopathic scoliosis, Eur J Hum Genet 11, 409-415
- Frey U.H., Hagen S., Bachmann H.S., Jürgen Peters J., and Siffert W., (2008). PCR-amplification of GC-rich regions slowdown PCR, J nat , 1312 - 1317
- Fujioka H., Ariga T., Horiuchi K., Otsu M., Igawa H., Kawashima K., Yamamoto Y., Sugihara T., Sakiyama Y., (2005) Molecular analysis of non-syndromic preaxial polydactyly: preaxial polydactyly type-IV and preaxial polydactyly type-I. Clin Genet 67,429-433
- Furga, S.A., And Unger, S., Nosology Group of the International Skeletal Dysplasia society(2007), Nosology And Classification of Genetic Skeletal Disorders, Amer J Med Genet Part A 143A:1-18.
- Giampietro P.F., (2012) Genetic Aspects of Congenital and Idiopathic Scoliosis. Scientica, 15,152365.
- Good C.R., (2009) The Genetic Basis of Adolescent Idiopathic Scoliosis, J Spin Rese Foun.
- Gorman k. F., Julien C ., And Moreau A. (2012) The genetic epidemiology of idiopathic scoliosis. Eur Spine J ,21,1905-1919
- Handforth J.R., (1950) Polydactylism of hand in southern Chinese. Anat Rec, 106,119-125
- Hartmann C., (2007) Skeletal development - wnts are in control, Mol Cells 24, 177-184
- Heuertz S., Le Merrer M., Zabel B., Wright M., Legeai-Mallet L., Cormier-Daire V., Gibbs L., Bonaventure J., (2006) Novel FGFR3 mutations creating cysteine residues in the extracellular domain of the receptor cause achondroplasia or severe forms of hypochondroplasia, Eur J Hum Genet 14, 1240-1247
- Horton W.A., (2006) Recent milestones in achondroplasia research, Am J Med Genet 140,166-169

- Hurst J.A., Firth H.V., Smithson S., (2005) Skeletal dysplasias, Semin Feta Neon Med 10,233-241
- James J.I.,And Lamb D.W., (1963) Congenital abnormalities of the limbs.J Practi 191:159-172
- Janicki J.A., and Alman B., (2007). Review of diagnosis and treatment. Paediatr Child Healt,12(9),771-776.
- Karkow D., Rimoin L.D., (2010).The Skeletal Dysplasias.GenetMed,2(6),327-341.
- Kornak U.,And Mundlos S., (2003).Genetic disorders of the skeleton: a developmental approach, Am J Hum Genet 73, 447-474
- Krakow D., Alanay Y., Rimoin L.P., Lin V, Wilcox W.R, Lachman R.S, Rimoin D.L (2009).Evaluation of prenatal-onset osteochondrodysplasias by ultrasonography: a retrospective and prospective analysis. Am J Med Genet 15, 1917-1924
- Laederich M.B and Horton W.A .(2012).FGFR3 targeting strategies for achondroplasia. Curr Opin Pediatr 22:516–523
- Laradi S., Tukel T., Khederi S., Shabbeer J., Erazo M.,Chkioua L., Chaabouni M, Le Merrer M., Rousseau F., Legeai-Mallet L., (1994). A gene for achondroplasia hypochondroplasia maps to chromosome 4p. Nat Genet 6,318-321
- Malik S.,Schott J.,Ali S.W.,Oeffner F., Amin-ud-Din M.,Ahmad W, Grzeschik K.H, Koch MC (2005). Evidence for clinical and genetic heterogeneity of syndactyly type I: the phenotype of second and third toe syndactyly maps to chromosome 3p21.31. Eur J Hum Genet 13, 1268-127411900.
- Martinez-Frias M.L., de Frutos C.A., Bermejo E., ECEMC Working Group, Nieto MA. 2010. Review of the recently defined molecularmechanisms underlying thanatophoric dysplasia and their potential therapeutic implications for achondroplasia. Am J Med Genet Part A 152A,245–255.
- Martínez N. A., Teixeira C. M., Saraiva M. H., Araujo A. H., (2001). Russel-Silver syndrome. An Esp Pediatr 54, 591-594

- Matise C.T., Chen F., Chen W., DeLaVega M.F., Hansen. M .,He.C., Hyland C.L.F., Kennedy G.C., Kong X.,Murray S., Ziegler J.S.,William C.L.,Stewart W., Buyske S., (2007) A second- generation combined linkage-physical map the human genome
- McInnes R.R., And Michaud J.L., (2008). Skeletal dysplasias and the growth plate. *ClinGenet* 73,24-30
- Montan A.M.,Tomatsu S.,Brusius A.,Smith M., Orii T., (2008). Growth charts for patients affected with morquio a disease. *Am J Med Genet* 146, 1286-1295
- Mortier G.R., (2001) The diagnosis of skeletal dysplasias: a multidisciplinary approach. *Eur J Radiol* 40, 161-167
- Muenke M., Gripp K.W.,McDonald-mcginn D.M., Gaudenz K.,Whitaker L.A., Bartlett S.P., Markowitz R.I., Robin N.H., Nwokorom., Mulvihill J.J., Losken HW, Mulliken J.B., Guttmacher A.E., Wilroy R.S., Clarke L.A, Hollway G., Ades L.C., Haan E.A., Mulley J.C., Cohen M.M., Bellus G.A., Francomano C.A., Moloney D.M., Wall S.A., Wilkie A.O., Zackai E.H., (1997) A unique point mutation in the fibroblast growth factor receptor 3 gene (FGFR3) defines a new craniosynostosis syndrome. *Am J Hum Genet* 60, 555-564
- Narayanan H.S., Mohan K.S.,Jayasimha N., Rao BS (1987). A clinical and biochemical study of the mucopolysaccharidoses. *Indian J Psychiatry* 29,123-126
- Neufeld E.F.,And Muenzer J., (2001) The mucopolysaccharidoses.In: Scriver CR, Beaudet AL, Sly WS, Valle D (eds). *The metabolic and molecular basis of inherited disease*. McGraw-Hill 3,3421-3452
- Noe E.J., Yoo H.W., Kim K.N., Lee S.Y., (2010). A case of thanatophoric dysplasia type Iwith an R248C mutation in the FGFR3 gene. *Korean J Pediatr* 12: 1022-1025
- Ocaka L., Zhao C.,Dowd J.O., Reed J.L., Ebenezer N.D., Brice G., Morley T., Mehta M., and Child A .H.,(2007) Assignment of two loci for autosomal dominant adolescent idiopathic scoliosis to chromosomes 9q31.2-q34.2 and 17q25.3-qtel. *J Med Genet* 45,87-92

Ornitz D.M., And Marie P.J., (2002) FGF signaling pathways in endochondral and intramembranous bone development and human genetic disease, *J Genes Dev* 16,1446-1465

Perez-Castro A.V., Wilson J., And Altherr M.R., (1997) Genomic organization of the human fibroblast growth factor receptor 3 (*fgfr3*) gene and comparative sequence analysis with the mouse *fgfr3* gene, *J Genom*, 41,10-16

Richette P., Bardin T., And Stheneur C., (2008) Achondroplasia: from genotype to phenotype. *Joint Bon Spin* 75, 125-130

Sambrook J., And Russell D., (2001) Molecular cloning, A laboratory manual cold spring harb protoc 3rd ed,476-48

Savarirayan R., And Rimoin D.L., (2002) The skeletal dysplasias, *Best Pract Res Clin Endocrinol Metab* 16,547-560

Schramm T, Gloning K.P., Minderer S., Daumer-Haas C., Hörtnagel K., Nerlich A, Tutschek B., (2009) Prenatal sonographic diagnosis of skeletal dysplasias. *Ultrasound Obstet Gynecol* 34, 160-170

Schweitzer D.N., Graham J.M., Lachman R.S., Jabs E.W., Okajima K., Przylepa K.A., Shanske A, Chen K, Neidich J.A., And Wilcox W.R., (2001) Subtle radiographic findings of achondroplasia in patients with crouzon syndrome with acanthosis nigricans due to an Ala391Glu substitution in FGFR3 Am J Med Genet 98,75-91

Shangguan L, Fan X., and Li M., (2008) Inheritance involved in the pathogenesis of idiopathic scoliosis. *J EXCLI* 7,104-114

Shanske A, Caride D.G, Menasse-Palmer L, Bogdanow A, Marion R.W (1997). Central nervous system anomalies in seckel syndrome: report of a new family and review of the literature, *Am J Med Genet* 70,155-158

Sheffield V.C., Nishimura D.Y., Stone E.M., (1995) Novel approaches to linkage mapping, *Curr Opin Genet Dev* 5, 335-341

Spranger J.W., (1977) Catabolic disorders of complex carbohydrates, Postgrad Med J 53, 441-449

Tavormina P.L., Bellus G.A., Webster M.K., Bamshad M.J., Fraley A.E., McIntosh I., Szabo J., Jiang W., Jabs E.W., Wilcox W.R., Wasmuth J.J., Donoghue D.J., Thompson L.M., Francomano C.A., (1999) A novel skeletal dysplasia with developmental delay and acanthosis nigricans is caused by a Lys650Met mutation in the fibroblast growth factor receptor 3 gene, Am J Hum Genet 64, 722-73

Trantirkova, F.S., Wilcox, R.W., Krejci, P., (2012) Sixteen years and counting: the current understanding of fibroblast growth factor receptor 3 (FGFR3) signaling in skeletal dysplasias, Hum Mutat. 33(1), 29–41.

Trobisch P., Suess O., And Schwab F., (2010) Idiopathic scoliosis.. Dtsch Arztbl Int . 107(49), 875-84

Trotter T.L. And Hall J.G., (2005) Health supervision for children with achondroplasia. J Pediatr , 116, 771-783

Tuysuz, B., (2004) A new concept of skeletal dysplasias, Turk J Pediatr, 46, 197-203

Vajo Z., Francomano C.A., Wilkin D.J., (2000) The molecular and genetic basis of fibroblast growth factor receptor 3 disorders: the achondroplasia family of skeletal dysplasias, Muenke craniostenosis, and Crouzon syndrome with acanthosis nigricans, J Endocr Rev, 21, 23-39

Warman M.L., Cormier-Daire V., Hall C., Krakow D., Lachman R., Lemerrer M., Mortier G., Mundlos S., Nishimura G., Rimoin D.L., Robertson S., Savarirayan R., Sillence D., Spranger J., Unger S., Zabel B., And Superti-Furga A., (2010) Nosology and classification of genetic skeletal disorders: 2010 Revision. Am J Med Genet, 155, 943-968

Wise C A., Gao X., Shoemaker S., Gordon D., and Herring J.A., (2008) Understanding Genetic Factors in Idiopathic Scoliosis, a Complex Disease of Childhood. J Curr Geno, 9, 51-59

Xue Y., Sun A., William R., Wilcox P., Mekikian B., Martin J., Rimoin L. D., Lachman S.R., (2014) FGFR3 mutation frequency in 324 cases from the International Skeletal Dysplasia Registry. *Am J Med Genet*, 155, 943-968

Zelzer B., Olsen B.R., (2003) The genetic basis for skeletal diseases. *Nature*, 423, 343-348

Zhang S., Zhou X., Ren X., Wang T.T., Yuan M.X., Wang Q., Liu J., Liu Mu., (2007) Ser217Cys mutation in the Ig II domain of FGFR3 in a Chinese family with autosomal dominant achondroplasia. *Chin Med J*, 120, 1017-1019

 Turnitin Originality Report

**Skeletal Dysplasia** by Yasmin Hashim

From thesis (Yasmin)

Processed on 21-Feb-2016 18:49 PKT  
ID: 634645479  
Word Count: 6790

Similarity Index	Similarity by Source
6%	Internet Sources: 0% Publications: 3% Student Papers: N/A

**sources:** 

- 1** 3% match ()  
<http://edrv.endojournals.org/cgi/content/full/21/1/23> <http://int-edrv.endojournals.org/cgi/content/full/21/1/23>
- 2** 3% match (Internet from 17-May-2014)  
<http://fu-gu.net/News/140.html>

**paper text:** 

**INTRODUCTION** The human skeleton is an endoskeleton composed of bones (206), cartilage and three types of cells, osteoblasts, osteoclasts and chondrocytes. Bone is a type of mineralized connective tissue that undergoes a process of renewing. During this process, old bones are destroyed and new ones are formed. Cartilage is an elastic type of connective tissue that constitutes the parts of the skeleton that can't be totally rigid, due to the necessity of body movements (Savarirayan and Rimoin, 2002). The human skeletal system has two sub division, axial and appendicular skeleton. The axial skeleton consists of 80